EGG-TMI-8020

Idaho
National
Engineering
Laboratory

Managed
by the U.S.
Department
of Energy

EGG-TMI-8020
April 1988

INFORMAL REPORT

ASSESSMENT OF TMI-2 PLENUM ASSEMBLY DAMAGE

P. Kuan

EG&G Idaho

Work performed under
DOE Contract
No. DE-AC07-76ID01570

EGG-TMI-8020

ASSESSMENT OF TMI-2 PLENUM ASSEMBLY DAMAGE

P. Kuan

Published April 1988

EG&G Idaho, Inc.
Idaho Falls, Idaho 83415

Prepared for the
U.S. Department of Energy
Idaho Operations Office
Under DOE Contract No. DE-AC07-76ID01570

ABSTRACT

This report attempts to explain the damage observed in the TMI-2 plenum assembly as a result of the 2-B primary coolant pump transient during the March 28, 1979 accident. It is conjectured that due to variations in the flow resistance toward the periphery of the upper plenum, hot gas flow during the pump transient split into two streams directed toward the north and the south quadrants of the upper plenum where observed damage occurred. Steam generation during the pump transient is calculated from system pressure response and the deduced flow rate is used in the calculations of heat transfer to the plenum assembly. Using the maximum average temperature (2000 K) attained by the particles in the upper core debris bed as the temperature of the gas exiting the core, the results of the calculations show that the thin structures at the lower end of the plenum assembly would have been melted, while the relatively thick structures would have been partially ablated, consistent with the observed damage. The calculations also show that without an appreciable amount of hydrogen present in the gas stream, melting in the plenum assembly would have been more extensive than observed. The presence of hydrogen could explain the inhomogeneity in the oxidation state of the plenum assembly structures. Energy balance considerations point to the rapid oxidation of zircaloy during the pump transient, which would have been a source of hydrogen and would have provided the energy required to maintain the high gas temperature.

ACKNOWLEDGMENTS

The author would like to thank Mike Martin for supplying information on the TMI-2 plenum assembly damage as observed in April 1984, prior to compiling it into a report. Specifically, Figure 8 (damage conditions on the underside of the plenum assembly as observed in April 1984), and Figures 12 and 13 (photo montages of the damaged L-10 and K-9 grid positions, respectively) are attributable to Mike. A panoramic view of the damage pattern, as given in the various figures in the report, was first constructed by A. Takazawa from videotape recordings and was subsequently rendered into excellent computer graphics by Mary Harris. Special thanks are extended to Gerry Reilly and Christine White, who prepared most of the drawings and plots in the report. Their dedicated efforts have made possible the timely publication of the report.

CONTENTS

ABSTRACT ii

ACKNOWLEDGMENTS iii

1. INTRODUCTION 1

2. PLENUM ASSEMBLY GEOMETRY 5

2.1 Upper Grid 5

2.2 Plenum Cylinder 8

2.3 Plenum Cover 10

2.4 Control Rod Guide Assemblies 12

2.5 Plenum Assembly Mass Summary 13

3. OBSERVED PLENUM ASSEMBLY DAMAGE AND DAMAGE MECHANISM 17

4. THERMAL-HYDRAULICS DURING THE 2-B COOLANT PUMP TRANSIENT 30

4.1 Heat Transfer to the B Steam Generator 30

4.2 Thermal-Hydraulics of the Primary System Fluid 34

4.3 Hot Gas Generation in the Reactor Core 42

5. PLENUM ASSEMBLY HEATING CALCULATIONS 51

5.1 Model Geometry 51

5.2 Heat Transfer Correlations and Parameters 55

5.3 Temperature and Melt Distributions 58

6. CONCLUSIONS 65

7. REFERENCES 69

FIGURES

1. General arrangement of TMI-2 reactor vessel and internals 2

2. Plenum assembly with a typical control rod guide assembly 6

3. Control rod guide assembly arrangement above upper grid 7

4. Upper grid unit cell structure 9

5. Azimuthal locations of main flow holes in the plenum cylinder 11

6. Lower end of a control rod guide assembly 14

7. Cast support plate which secures the "C" and split tubes inside the tubular housing of the control rod guide assembly 15

8. Damage conditions on the underside of the plenum assembly as observed in April 1984 18

9. Damage conditions on the underside of the plenum assembly as of November 1984 19

10. Damage pattern on the underside of the plenum assembly 21

11. Locations of missing upper end fittings on the underside of the plenum assembly 22

12. Damaged grid and guide structures over core position L10. Note the evidence of damage by foaming oxidation (irregular foamy appearance), melting (elongated frozen drops), and ablation (missing ribs along south side), as well as the melting of guide structures above the grid 24

13. Damaged grid structures over core position K9. While damage types are similar to those in Figure 12, the guide structures above the grid remain largely intact 25

14. Azimuthal locations of main flow holes in the plenum cylinder in relation to plenum assembly damage pattern 27

15. Steam generator showing position of level measurement in the downcomer 32

16. Steam generator B secondary side pressure during the 2-B pump transient 35

17. Steam generator B secondary side riser liquid level and measured downcomer liquid level during the 2-B pump transient 36

18. Mass partition between vapor and liquid on secondary side of B steam generator during the 2-B pump transient 37

19. Cumulative energy transfer to the B steam generator secondary side during the 2-B pump transient 38

20. Primary cooling system volume distribution. Volumes are in m^3 40

21. Primary system pressure during the 2-B pump transient 44

22. Primary system mass partition between vapor and liquid during the 2-B pump transient 45

23. Net energy transferred to the primary system fluid during the 2-B pump transient 46

24. Steam generation rate in the reactor core during the 2-B pump transient 48

25. Total energy transfer from the reactor core to the reactor cooling system during the 2-B pump transient 49

26. Heat transfer rate from the reactor core to the reactor cooling system during the 2-B pump transient 50

27. Model of a plenum assembly grid structure unit cell for thermal calculations 52

28. Calculated gas temperature distribution in the upper plenum during plenum assembly heating 64

TABLES

1. Plenum assembly mass distribution 16

2. Primary cooling system fluid parameters 43

3. Plenum assembly structure parameters for a unit cell 54

4. Plenum assembly heating for gas emissivity = 0.3 59

5. Plenum assembly heating for gas emissivity = 0.5 60

6. Plenum assembly heating for gas emissivity = 0.7 61

1. INTRODUCTION

During the TMI-2 accident on March 28, 1979, much of the reactor core was damaged, but damage to the plenum assembly appears minimal. The purpose of this report is to determine a mechanism that contributed to the limited plenum assembly damage in the presence of severe core damage. A general arrangement of the TMI-2 reactor vessel and internals, showing the relative positions of the core and the plenum assembly, is shown in Figure 1.

During the accident, approximately a third of the reactor core melted. Part of the melted core relocated to the core bypass region around the periphery of the core, part to the lower plenum, and the remainder solidified in the central region of the core, supporting a particle bed formed from shattered fuel and cladding.[1] Such an extensive melting of the core indicates that peak temperatures may have exceeded the melting point of the uranium dioxide fuel--about 3100 K. Examination of the particles from the particle bed shows that some may have reached the melting point of uranium dioxide, but the bulk average temperature of the particles probably only peaked in the neighborhood of 2000 K.[2]

Two principal damaged zones are observed in the plenum assembly at mid-radius locations on the underside of the upper grid, which holds down the fuel assemblies during power operation. The damage is recognized by partial melting, foamy oxidation, and discoloration of the stainless steel structures from excessive heating. The total area of the damaged zones comprises about 35% of the area of the bottom surface of the grid. The interior of the plenum assembly has not been examined except the lower end of the control rod guide assemblies viewed from the underside. Some melting of the thin structures inside these assemblies may have occurred where the grid ribs had been ablated, but the extent is unknown. Two control rod leadscrews were removed from the reactor vessel prior to any knowledge of plenum assembly damage and were examined metallographically. One of the leadscrews was from the radial center of the core (core position H8) and the other from close to the periphery (core position B8). No damage was observed at either location on the underside of the upper

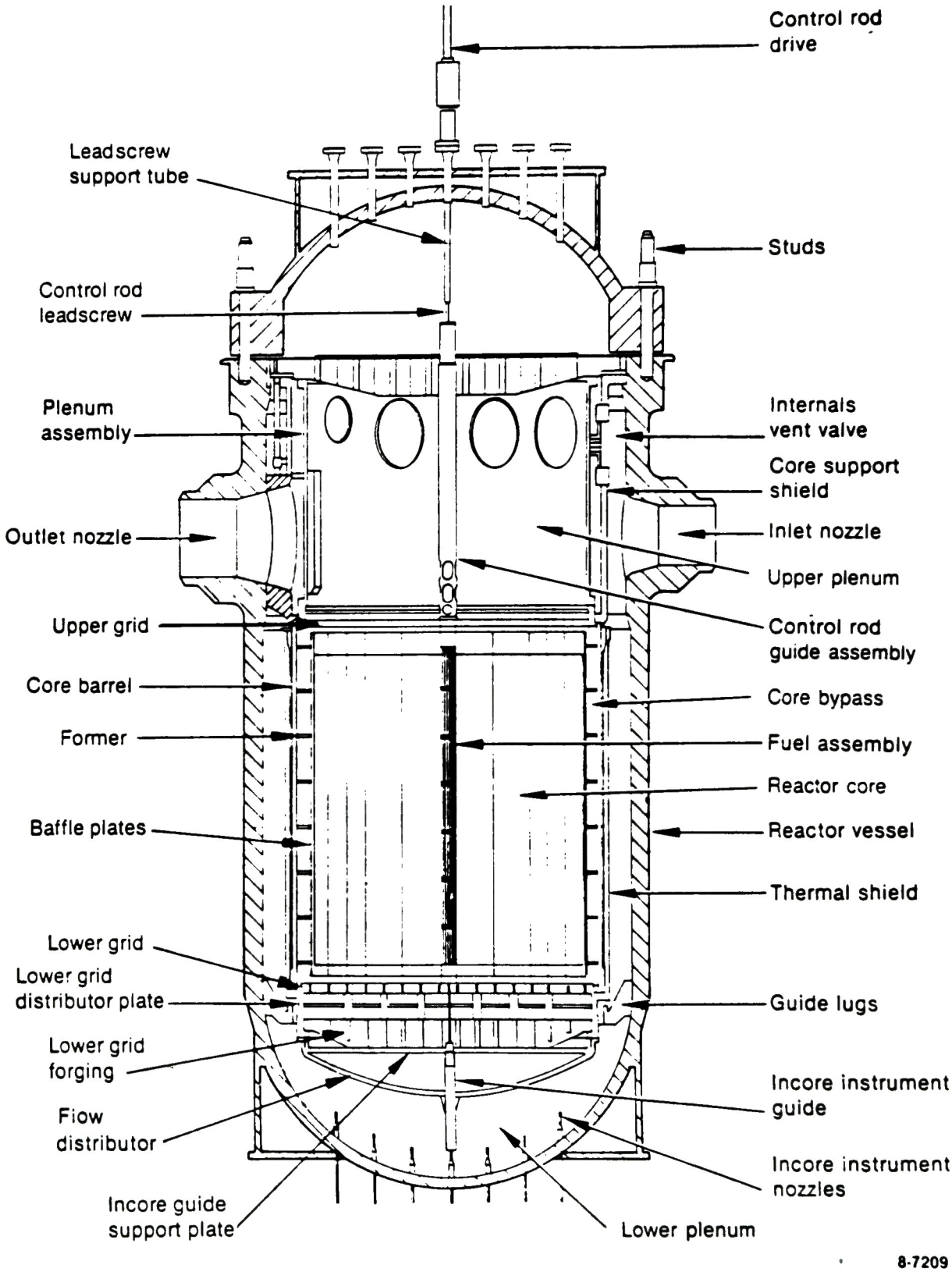

Figure 1. General arrangement of TMI-2 reactor vessel and internals.

plenum. This is consistent with the metallographic examination which showed that the maximum temperature of the examined leadscrews inside the upper plenum only reached 1255 K.[3]

The lack of extensive damage in the plenum assembly is in distinct contrast to the severe damage in the core. The upper plenum was directly above and in close proximity to the core and it is expected that the heating of the core would have been closely coupled to the heating of the plenum structures. It is especially intriguing when one considers that steel melts at about 1750 K, a temperature much lower than the peak temperatures attained by the particle bed directly below the plenum assembly.

There has been much interest in the phenomenon of natural circulation during the course of a severe light water reactor accident.[4] The main concern is that as the reactor core is uncovered, fluid circulation patterns may set up in the reactor vessel. Water is boiled off in the lower core; the steam picks up heat as it flows through the high temperature core and dissipates some of the heat in the upper plenum structures. The cooled gas sinks around the periphery of the core to complete the circulation loop. When such a loop is set up, a significant fraction of the core heat may be transferred to the plenum assembly, eventually causing the structures to melt. A mixture of molten steel and core debris may enhance fission product release during later phases of a severe accident as the molten corium comes in contact with concrete after vessel breach.[4] A similar natural circulation scenario may be envisioned for the reactor system cooling loops. In this case, some core heat is transferred to the steam generator tubes, which may eventually fail due to high temperature and create a direct path for fission product release to the environment.

Natural circulation loops around the primary cooling system during the TMI-2 accident were never strong enough to transfer much of the core heat to thermally damage the steam generator structures. Damage to the plenum assembly, though quite limited as observed so far, may have been caused by in-vessel natural circulation during the high temperature phase of the

accident. However, the existence of two damage zones away from the radial center of the plenum assembly is unexpected from a perspective of natural circulation. Since the core was hottest in the radial center, hot gas would have risen from that region to the upper plenum and caused the most damage at the center of the upper grid. Also, the inhomogeneity over short distances in thermal damage, as well as in the degree of oxidation of the steel, would indicate a damage mechanism that has a short timescale rather than one of natural circulation. Once set up, natural circulation would persist for a relatively long period of time until either the heat source (core) or sink (plenum assembly) was removed.

As the reactor vessel is being defueled and while the plenum assembly is resting in the refueling canal, the full extent of the plenum assembly damage is still unknown. The mechanism for the observed damage remains unclear and any explanation carries the burden of controversy. Nevertheless, this study intends to explore the conditions under which the plenum assembly was damaged and predict the extent of damage in the unobserved or unobservable interior of the plenum assembly. Lacking a comprehensive calculation of the thermal and hydraulic interactions, this study is restricted to a brief period in the accident during which the damage was hypothesized to have occurred. This period is when the 2-B reactor coolant pump was momentarily turned on and delivered a large amount of water to the core in the first few seconds of its operation.

The rest of the report is organized as follows. Section 2 describes the plenum assembly geometry in some detail so as to identify flow paths and perform calculations of the heating of the plenum assembly structures. Section 3 presents the observed plenum assembly damage and argues for the 2-B pump transient as a possible damage mechanism. Section 4 examines the thermal-hydraulic conditions during the 2-B pump transient and deduces the flow rates to the upper plenum during that period. Based on indirect knowledge of the average peak temperatures attained in the core particle bed and the flow rates deduced in Section 4, calculations of heat transfer to the plenum assembly structures are performed and the results presented in Section 5. Conclusions are given in Section 6.

2. PLENUM ASSEMBLY GEOMETRY

This section describes the geometry of the as-designed plenum assembly structure. The description will be in general terms, identifying the major components. Dimensions of structures are extracted from miscellaneous drawings of the reactor vessel.

The plenum assembly, once assembled, is a structure which can be moved as an integral piece. Its main components are: (a) the (core) upper grid, (b) plenum cylinder, (c) plenum cover, which consists of interweaving plates forming a square lattice and a cover plate, and (d) the control rod guide assemblies which extend from the upper grid to some 19 inches above the cover plate. The plenum cylinder, which has flanges at both ends, is bolted at its lower end to the upper grid and at its upper end to the plenum cover.

The TMI-2 core consists of 177 fuel assemblies, corresponding to 177 upper grid positions. The core is arranged in such a way that there are 40 peripheral assemblies. Of the remaining 137 assemblies, 69 have either control or axial power shaping rods whose movements are controlled by leadscrews and guided by the control rod guide assemblies. These guide assemblies are arranged in a checkerboard pattern above the upper grid. A schematic drawing of the plenum assembly is shown in Figure 2, and the positions of the control rod guide assemblies are shown in Figure 3.

The major components of the plenum assembly are described in the following subsections.

2.1 Upper Grid

The upper grid is used to position the fuel assemblies to prevent lateral movement during operation. The grid assembly consists of a rib section whose periphery is bolted to a ring forging which is attached to the plenum cylinder. The grid consists of square openings above the fuel

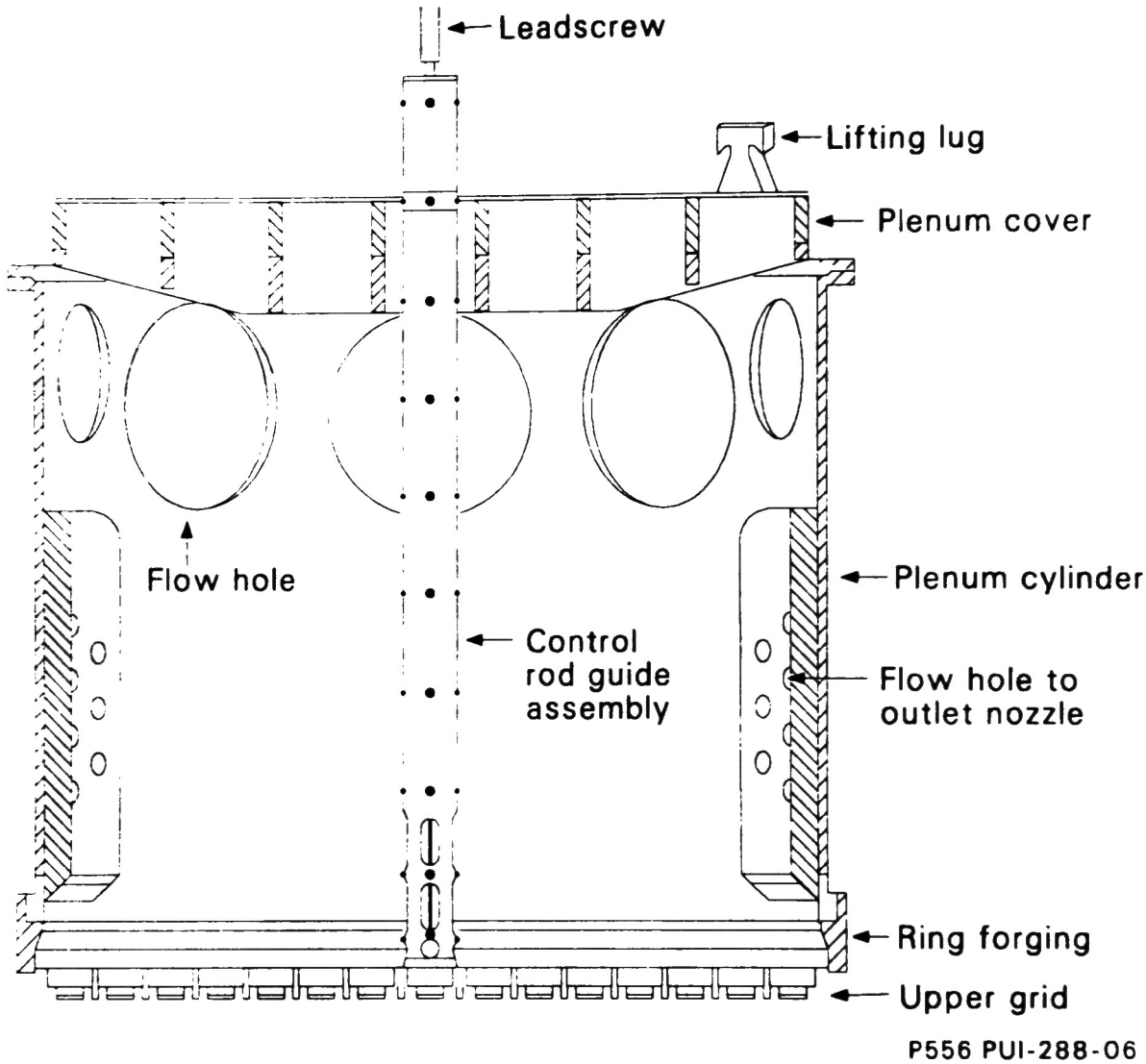

Figure 2. Plenum assembly with a typical control rod guide assembly.

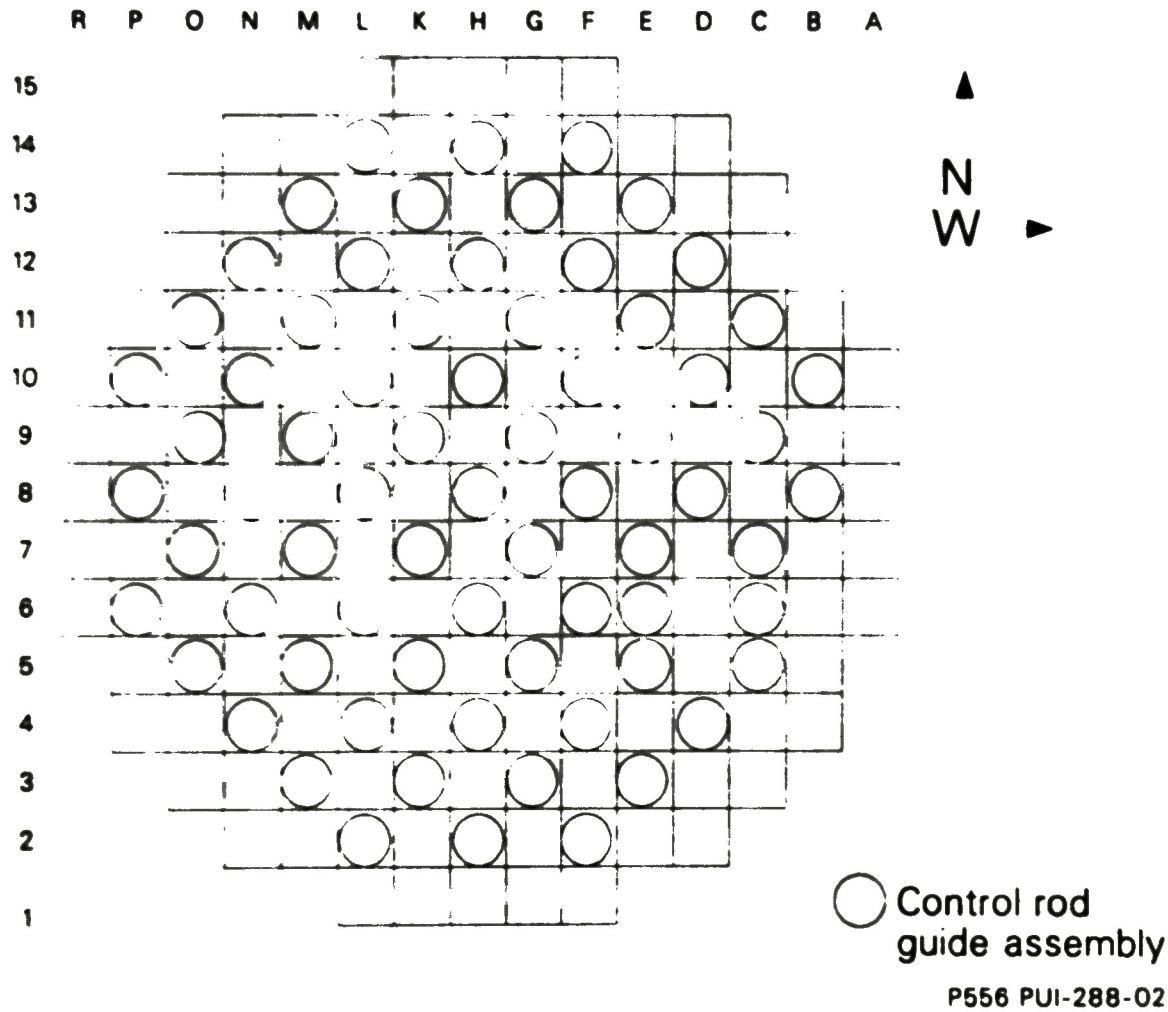

Figure 3. Control rod guide assembly arrangement above upper grid.

assemblies. The rib section is 3 inches thick and the ribs making up the boundaries of the square holes are 1 inch in width. The ribs themselves are not in direct contact with the fuel assemblies. Grid pads, 5-1/2 inches long, 2 inches thick, and slightly wider than the ribs, are attached to the ribs. These pads fit in-between the fuel assemblies and press down against the spring hold-down rings in the fuel assembly upper end fittings. Figure 4 shows a unit cell of the rib structure above a typical assembly.

In addition to positioning the fuel assemblies, the grid also provides support to the control rod guide assemblies, which are attached to the ribs with flanges at alternate grid positions.

Based on a nominal density of 500 lb/ft^3 for stainless steel (density used for all subsequent mass calculations), the calculated mass of the rib section is 3814 lbs; pads, 1461 lbs; and the ring forging 2398 lbs--making the total mass of the upper grid assembly 7673 lbs.

2.2 Plenum Cylinder

The plenum cylinder is a hollow, thin-walled steel cylinder with flanges at both its lower and upper ends for attachment to the upper grid and the plenum cover, respectively. The height of the cylinder is a little over 102 inches, and its internal diameter is 127 inches, with a wall thickness of 1-1/2 inches. Besides serving as a structural component for joining the upper grid and the plenum cover, the plenum cylinder also serves as a guide for balanced fluid flow from the core to the outlet nozzles. This is accomplished with large holes in the cylinder wall about three-quarters of its height above the lower end. The holes are of two sizes--six having a diameter of 34 inches and four having a diameter of 22 inches. Twenty-four holes are also drilled in the plenum cylinder at each of the two positions of the outlet nozzles, but these are only 4-1/2 inches in diameter and are further restricted by 3-inch holes in the reinforcing plates placed inside the cylinder at these locations.

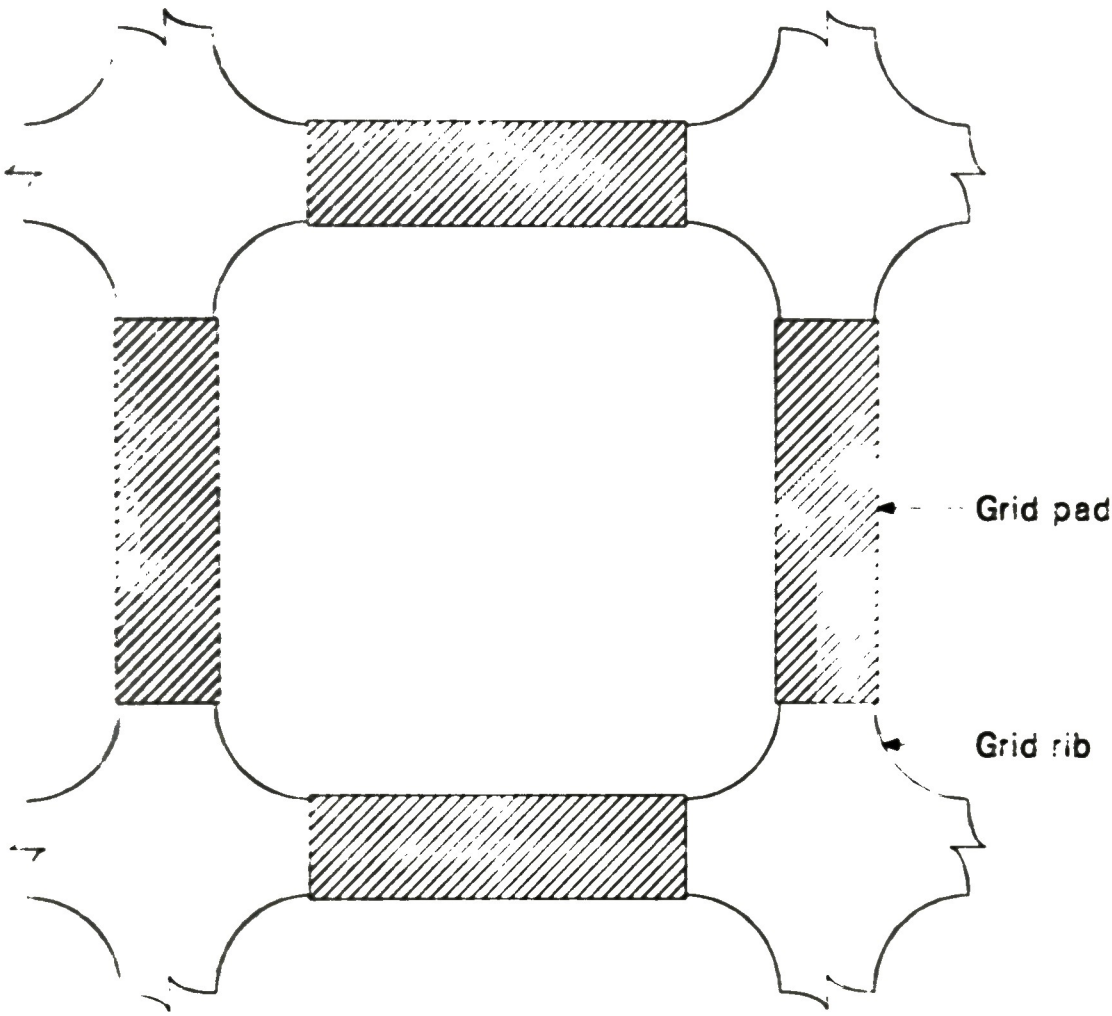

Figure 4. Upper grid unit cell structure.

Although these smaller holes provide shorter paths for the flow from the reactor core to the outlets (equivalent to a 14.7-inch hole at each nozzle), they are not expected to carry much of the flow as the larger holes would because of their size. The positions of the flow holes may have affected the damage pattern in the plenum assembly. This is discussed in Section 3 on the observed plenum assembly damage. The positions of these holes around the circumference of the plenum cylinder are shown in Figure 5.

The mass of the flanged plenum cylinder is calculated to be 17,310 lbs, and that of the two reinforcing plates at the positions of the nozzles, 5845 lbs, making the total plenum cylinder mass 23,155 lbs.

2.3 Plenum Cover

The plenum cover grid structure is constructed from 20 2-inch flat plates; 10 are placed parallel at equal spacings, and the other 10, also placed parallel at equal spacings, intersect the first set at right angles, to form a square lattice. These openings accommodate the 69 control rod guide assemblies. The top of the grid structure is covered with a thin circular plate 1/2 inch thick and 124 inches in diameter, with 69 matching holes for penetration of the control rod guide assemblies. When the plenum cover is attached to the plenum cylinder (inside diameter 127 inches), a flow gap of 1-1/2 inches is formed between the plenum cover plate and the plenum cylinder. This allows some flow from the upper plenum to the vessel upper head. Another flow path is through the inside of the control rod guide assemblies. These are the only two direct flow paths from the upper plenum to the upper head. Because these flow areas are relatively small compared to those of the flow holes in the plenum cylinder, and because there are no flow outlets in the upper head other than the downward path to the outlet annulus around the plenum cylinder, these flows to the upper head are insignificant.

During plenum removal in May 1985, no damage was observed on the plenum cover. Metallographic examination of two leadscrews indicates that the maximum temperature reached in this region during the accident was

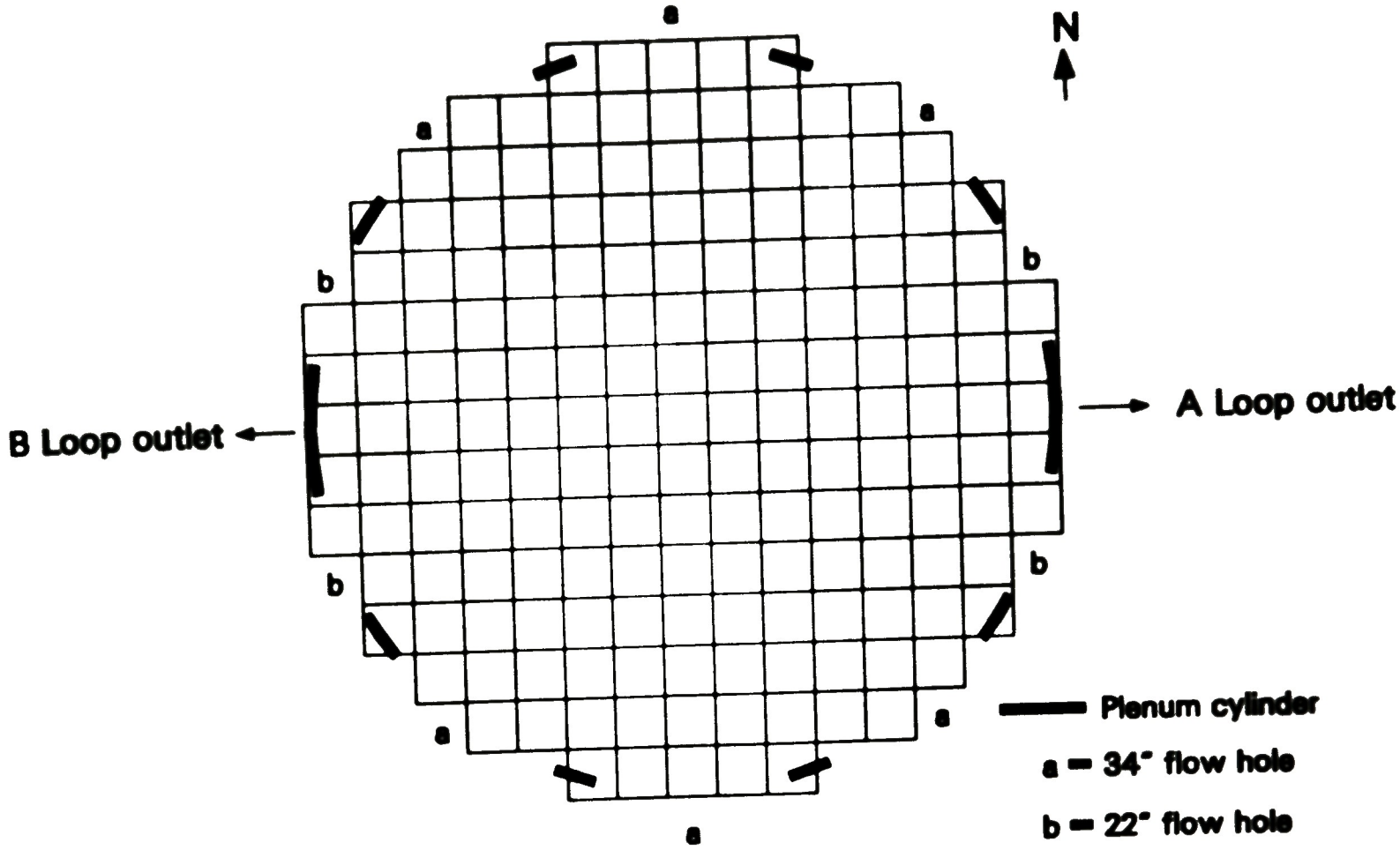

P656 PUI-288-05

Figure 5. Azimuthal locations of main flow holes in the plenum cylinder.

only about 700 K. Therefore, it is most likely that the plenum cover was indeed undamaged, and accordingly, the plenum cover will be omitted from the subsequent heatup calculations.

The mass of the plenum cover, including ribs, cover plate, flanges, lifting lugs, and weld filler material, is calculated to be 27,760 lbs.

2.4 Control Rod Guide Assemblies

The control rod guide assembly is a fairly complicated structure. It consists of an outer tubular housing, 8-5/8 inch OD and 8 inch ID along most of the tube, but narrowing to about 8-1/2 inch OD near the plenum cover. The tubular housing is flanged at its lower end and is bolted to the upper grid ribs. It penetrates the cover plate to which it is welded and protrudes to a height of about 19 inches above the cover plate. Inside the housing are the guide structures. These consist of 12 slotted tubes ("C" tubes) and four sets of tube sectors (split tubes). These guide the up-down motion of the control rod spider and the 16 control rods in each control assembly. They are brazed to 10 cast support plates along the length of the control rod guide assembly. These 3/4 inch thick plates are bolted to the tubular housing. In addition to these structures, the leadscrew travels along the axis of the assembly. After scram, the leadscrew occupies the entire length of the guide assembly. As mentioned earlier, the total number of guide assemblies is 69, one for each of the control or axial power shaping rod assemblies. These assemblies are arranged in a checkerboard pattern above the core upper grid.

Flow from the core can enter the control rod guide assemblies but most of it is not expected to travel the full length of the assemblies to the vessel upper head. There are three sets of holes (four in each), near the bottom end of the tubular housing below the third support plate at 27-1/2 inches. The lowest set of holes are circular (3 inches in diameter), and the two higher sets are elongated to about 9 inches. Due to the obstruction by the guide structures, leadscrew, and support plates, most of the flow entering the control rod guide assembly is expected to

exit to the plenum through these holes and a negligible fraction may exit the top of the guide assembly to the upper head.

The lower end of the control rod guide assembly is shown in Figure 6 and a plane view of the support plate and the guide structures is shown in Figure 7.

The mass of each tubular housing is calculated to be 304 lbs and the other structures 160 lbs, making a total mass of 464 lbs for a single assembly. The total mass of the 69 assemblies is 32,016 lbs.

2.5 Plenum Assembly Mass Summary

The mass distribution of the plenum assembly is summarized in Table 1. As shown in the table, the total design mass of the plenum assembly, according to the present calculation, is 90,604 lbs. The dry weight of the damaged assembly obtained during its lifting in May 1985, again assuming a density of 500 lb/ft^3 to correct for buoyancy in water, is 90,910 lbs.[5] The closeness in the calculated design mass and the measured mass of the plenum assembly indicates that significant melting the plenum assembly with attendant mass loss could not have occurred during the accident.

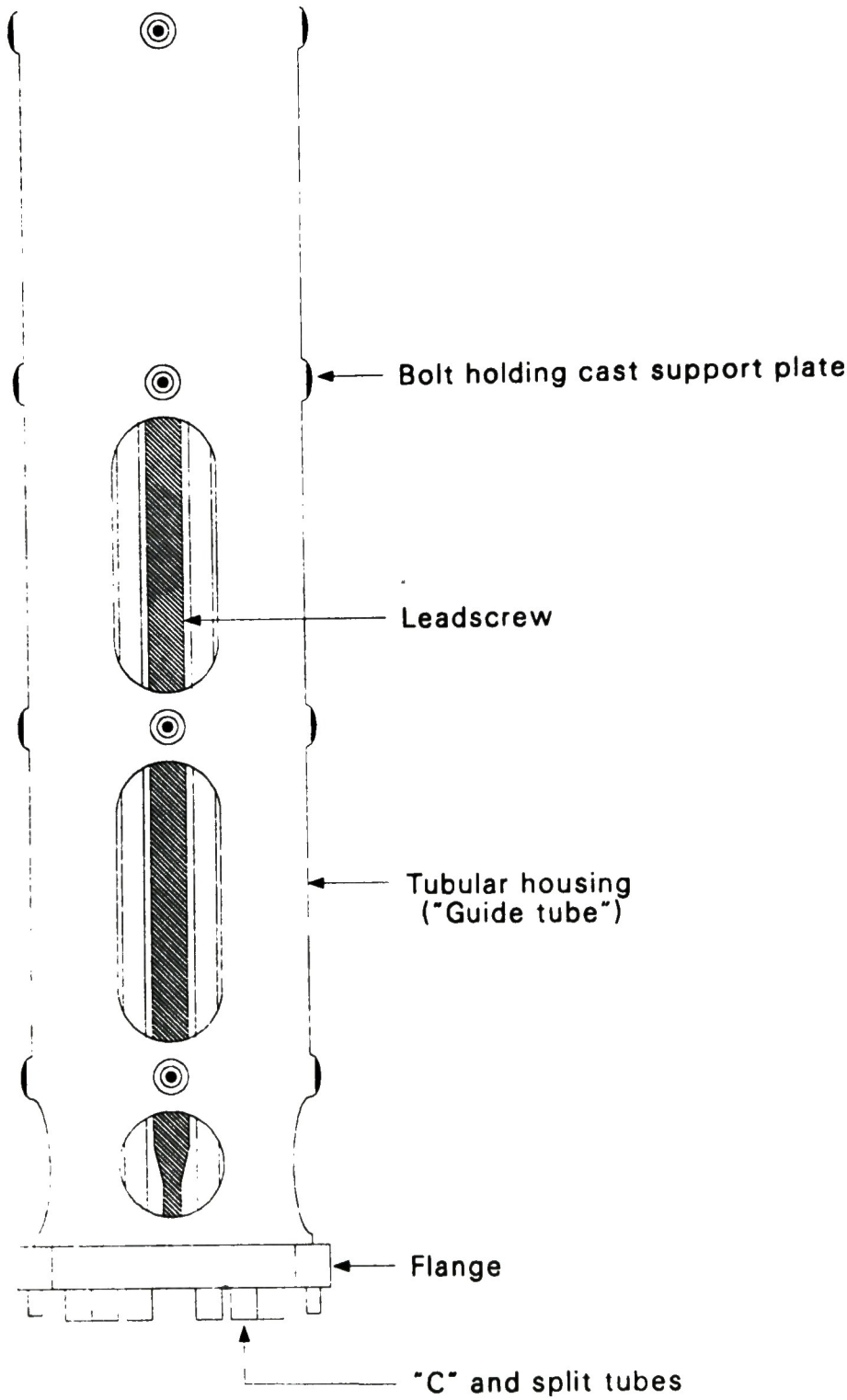

P556-WHT-288-04

Figure 6. Lower end of a control rod guide assembly.

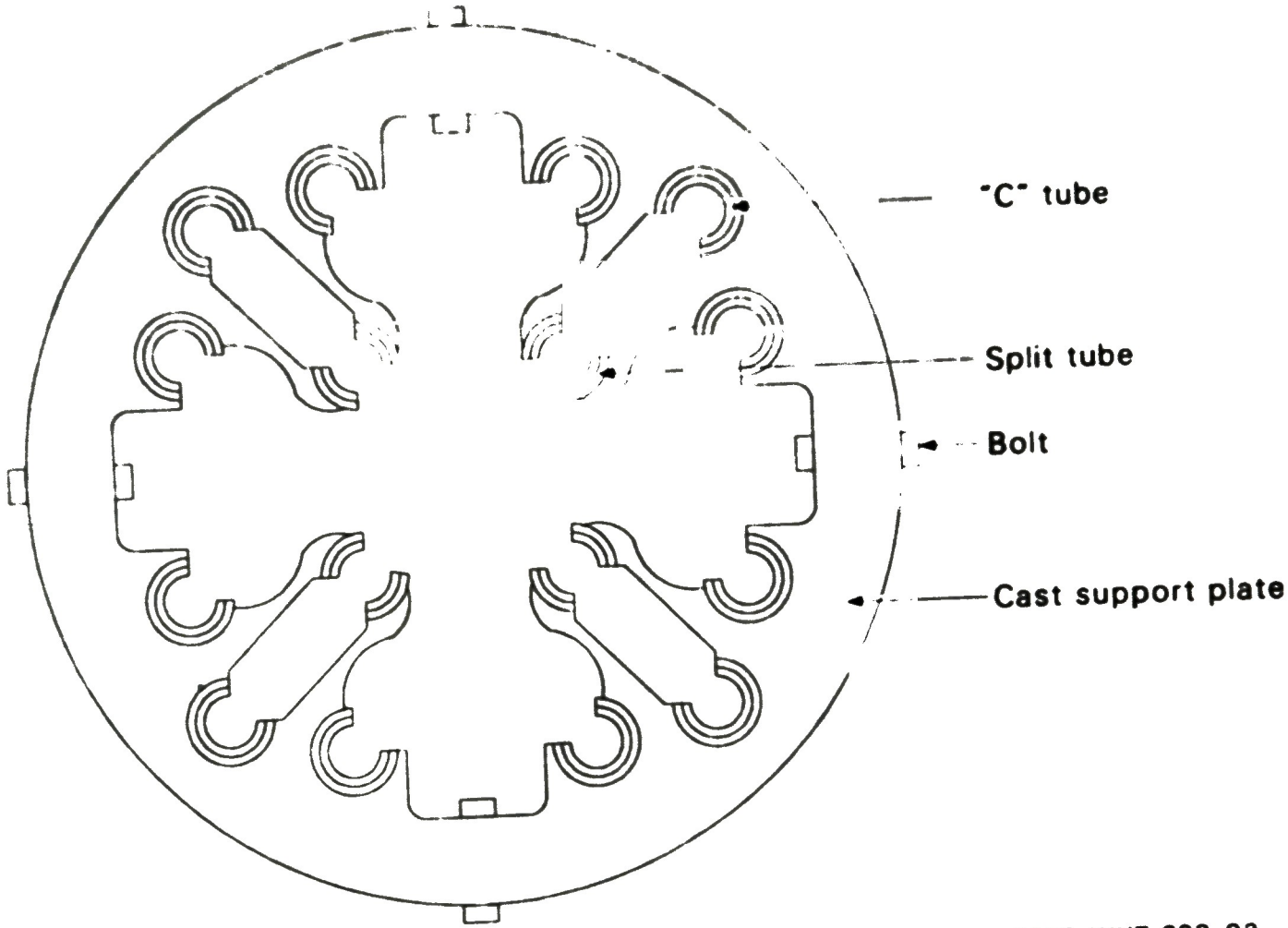

Figure 7. Cast support plate which secures the "C" and split tubes inside the tubular housing of the control rod guide assembly.

TABLE 1. PLENUM ASSEMBLY MASS DISTRIBUTION

Structure	Mass (lbs)
Upper grid	7,673
Plenum cylinder	23,155
Plenum cover	27,760
Control rod guide assemblies	32,016
Total	90,604

3. OBSERVED PLENUM ASSEMBLY DAMAGE AND DAMAGE MECHANISM

The earliest observation of the damage to the plenum assembly was made in April 1984, with a video camera lowered through the H8 (core center) control rod guide assembly after the leadscrew had been removed. Except for the standing peripheral assemblies, a void existed in the upper part of the core where the rod bundles had disintegrated into a rubble bed. The existence of the void enabled the camera to swing laterally to obtain a panoramic view of the conditions on the underside of the plenum assembly. The results are graphically depicted in Figure 8.[6] Above the void, there were a large number of upper end fittings still attached to the underside of the plenum assembly, some partially damaged, some still intact. Where the end fittings were missing, partial damage and some melting of the upper grid were observed. So, it is likely that the missing end fittings had stuck to, or at, the upper grid but were later melted away. Due to the limited viewing angle, the full extent of the damage to the underside of the plenum assembly was not obtained.

After the in-core inspection in April 1984, the leadscrews were disengaged from the control rod spiders and were lifted above the top of the guide assemblies to facilitate reactor head removal. The fact that the leadscrews could be disengaged and lifted indicated that the leadscrews were not deformed to a point that significant interference of their movement occurred. Nevertheless, the extent of the damage to the leadscrews remains unknown.

With the leadscrews parked within the control rod drives, the reactor vessel head was removed in July 1984. Attempts were then made to dislodge any end fitting that was attached to the underside of the plenum assembly. Such efforts, together with video inspections, yielded the status of the upper end fittings in relation to the plenum assembly. This is shown in Figure 9.[7] The categories "not inspected" and "verified present" represent those end fittings that were still attached to standing fuel assemblies. These generally were located at the periphery of the core where comparatively little damage to the assemblies occurred. The category under "dislodged" represents those that could easily be knocked

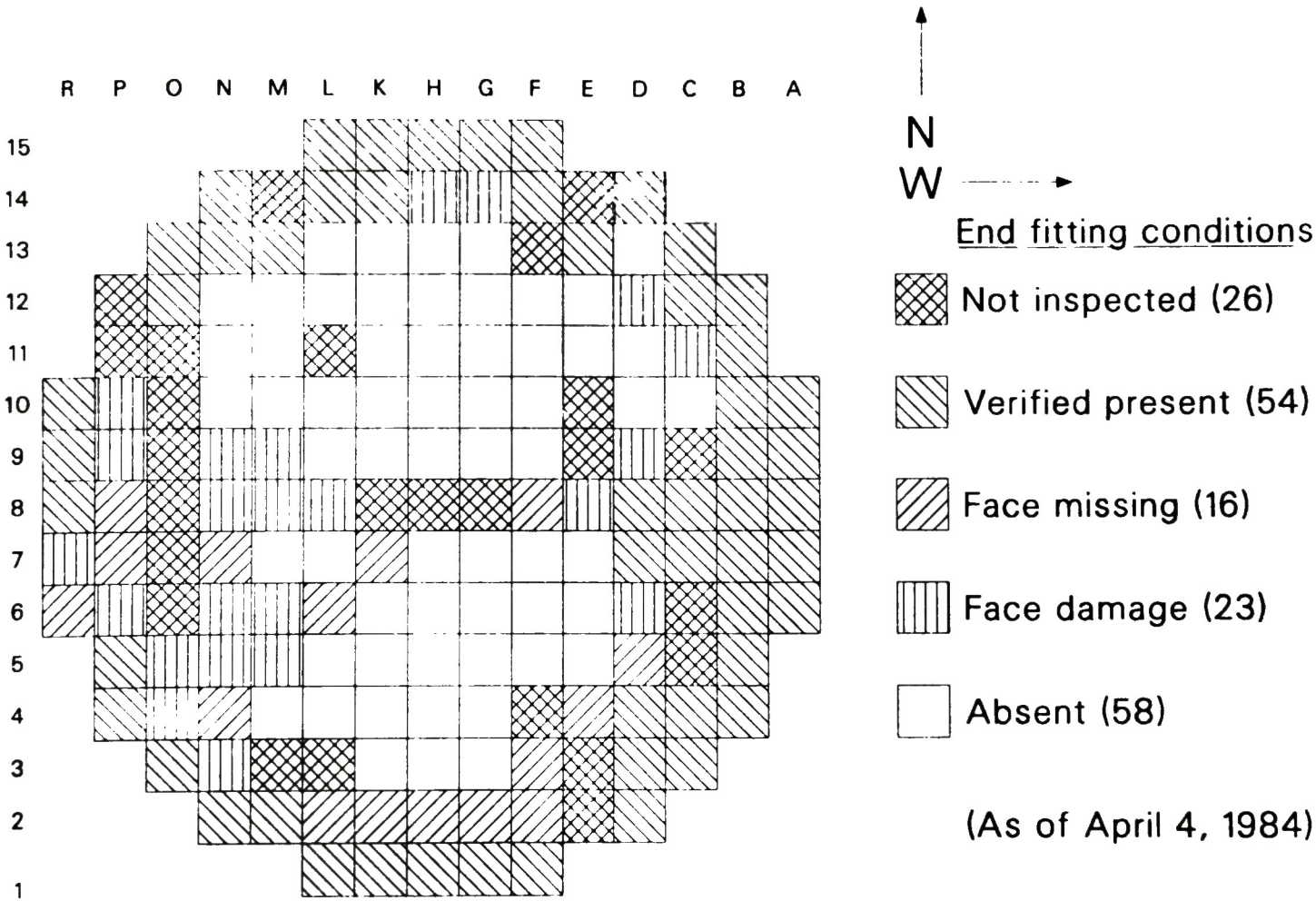

P556 PUI-288-04

Figure 8. Damage conditions on the underside of the plenum assembly as observed in April 1984.

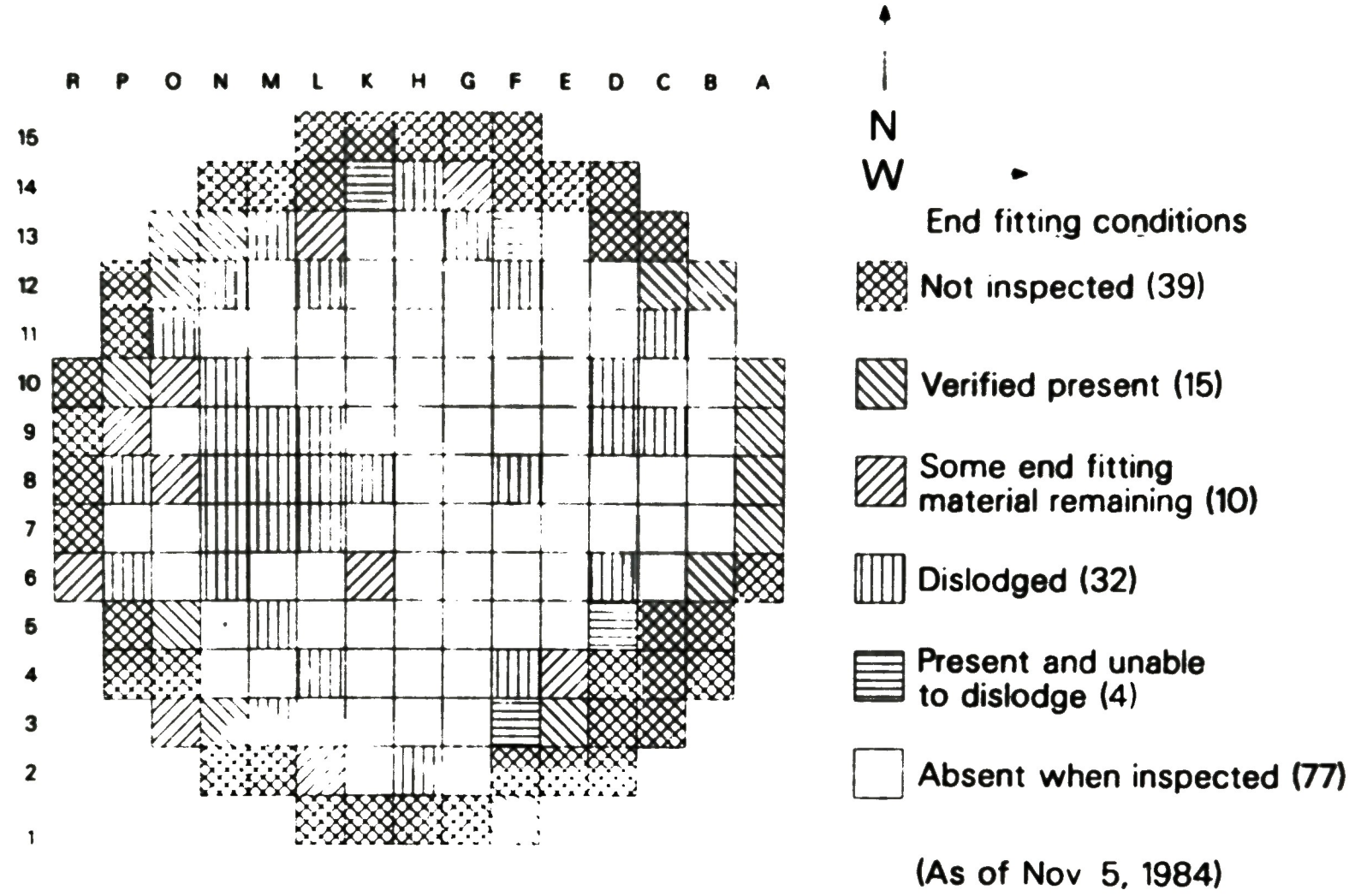

P556 PUI-288-03

Figure 9. Damage conditions on the underside of the plenum assembly as of November 1984.

off from the plenum assembly by a slide hammer. These were slightly damaged end fittings that were stuck to the upper grid. The categories "some end fitting material remaining" and "present and unable to dislodge" represent those that were partially melted, severely deformed, and probably were welded to the upper grid during the accident. The category "absent when inspected" represents those grid positions that had no end fitting attached to them. In general, the conditions shown in Figure 9 were essentially the same as those shown in Figure 8, indicating that the configuration was fairly stable and represented the end-state damage from the accident in 1979. Any minor discrepancies may have been caused by the difficulties of the observations and the independent judgments of the observers.

A full view of the damage to the underside of the plenum assembly was not obtained until the plenum assembly was lifted from the reactor vessel on May 15, 1985. Video monitoring was conducted during the removal process and the information stored on a GPUN video tape labeled "Plenum Lift Entry No. 613, May 15, 1985." No discernible damage was observed at the top of the plenum assembly and around the plenum cylinder. The underside of the upper grid, however, showed considerable damage. The damage pattern is shown in Figure 10.[8]

The most striking feature of the damage to the underside of the upper grid is the existence of two distinct damage zones at mid-radius locations in the north and south halves of the cross section. As shown in Figure 11, these are precisely the two zones where the upper end fittings were missing during earlier observations. Within the damage zones, some melting of the upper grid pads is evident. In a few places, such as the boundary between the H11 and H12 grid positions, the ribs are missing, apparently having been melted away. At most positions within the damage zones, the structures inside the control rod guide assemblies also were missing and apparently melted away. In most places, however, the grid structure remains clearly recognizable. The appearance of the damaged structures is extremely nonuniform. Some show ablation at the edges, making the damaged ribs thinner than the undamaged ones, but most of the

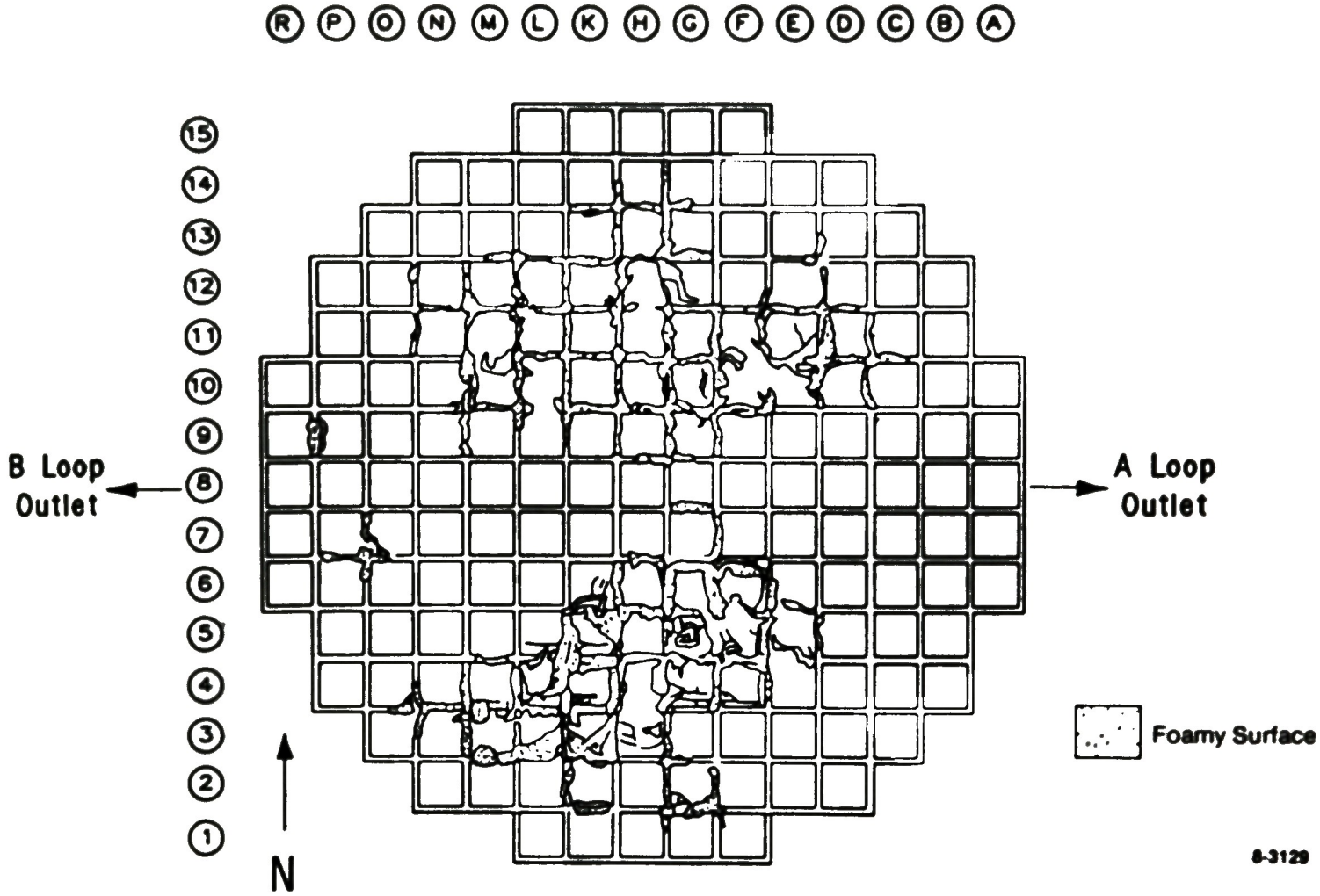

Figure 10. Damage pattern on the underside of the plenum assembly.

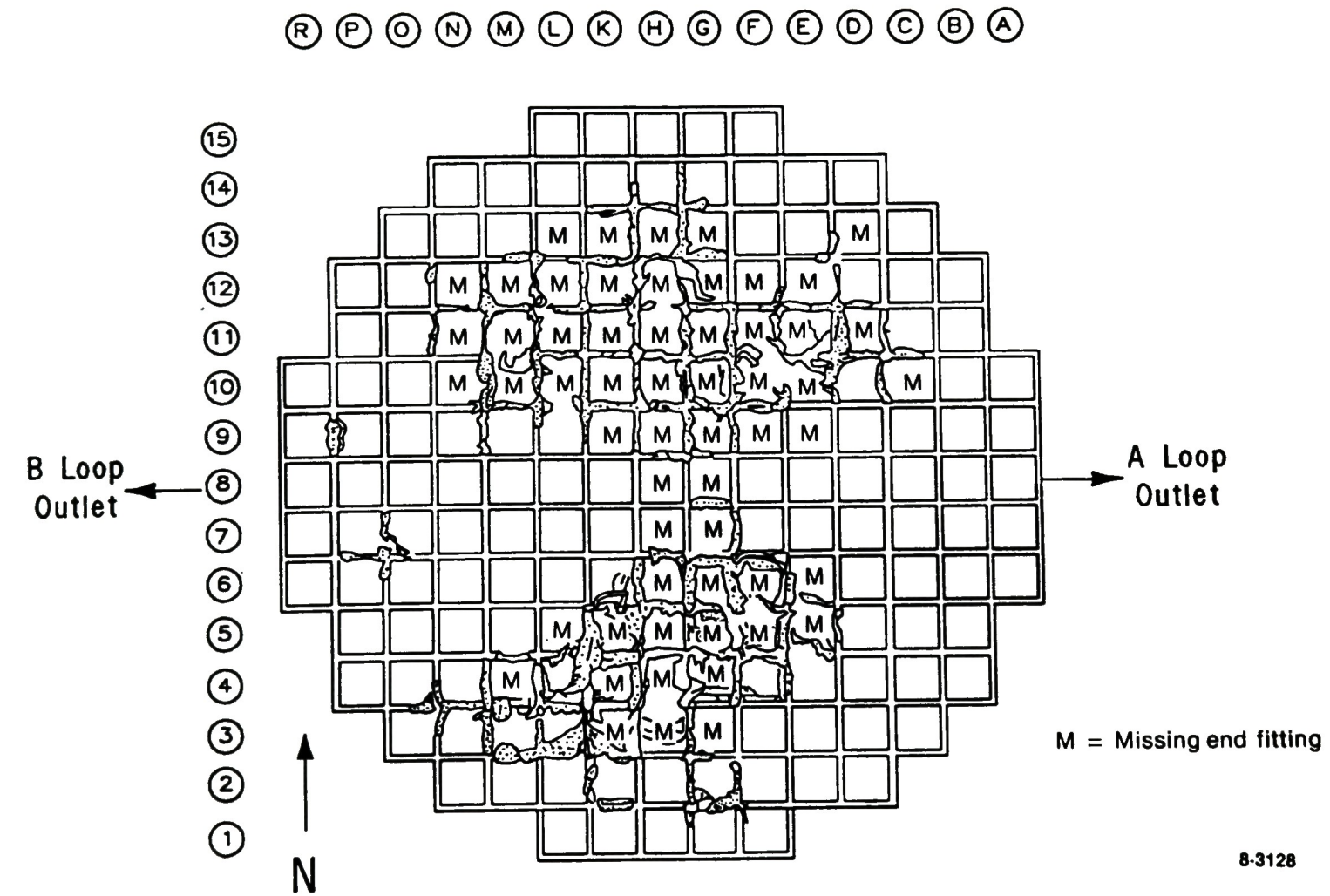

Figure 11. Locations of missing upper end fittings on the underside of the plenum assembly.

remains of the damaged ribs show dimensional growth and loss of original geometry, caused by either foaming oxidation or accumulation of previously molten material which had dripped from above.

The damage characteristics can change abruptly from one rib to its nearby neighbor. One rib could be severely deformed or missing, while a nearby rib could have suffered only minor ablation. One rib could be extremely foamy, porous, and apparently highly oxidized, while another could be glazed with a layer of solidified melt. At the transition between the damaged and the undamaged zones, the contrast can be quite startling. At positions where the partially damaged end fittings were stuck to the upper grid, some of the thin structures appear foamy or to have been melted, while other equally thin or thinner structures a few inches away remain intact. Similar nonuniformity in damage exists in the upper grid. For example, the rib between the L10 and L9 positions is missing (apparently melted away), while the structures at the L8 position have no discernible damage. A second example is the K9 position. Its rib pads toward the damaged zone to the north are very foamy in appearance, while the structures inside the control rod guide assembly were only slightly ablated. Away from the damage zone, the adjacent K8 position has no discernible damage. Montages of the L10 and K9 positions, made from video images taken before leadscrew removal, are shown in Figures 12 and 13, respectively. Both are control positions. Note that the guide structures above the L10 position appear to be mostly melted, including the tip of the leadscrew, while those above the K9 position are clearly visible.

The nonuniformity in damage to the underside of the assembly plenum suggests that hot gas flow to the upper plenum must have been nonuniform. First, the flow of hot gas obviously must have been restricted to the damaged zones. Second, within each flow path the composition of the gas must have varied from a strongly oxidizing atmosphere (steam) to a somewhat reducing atmosphere (partially hydrogen) over distances on the order of a fuel assembly width or less. Third, the flow of hot gas through the observed damage zone must have been of relatively short

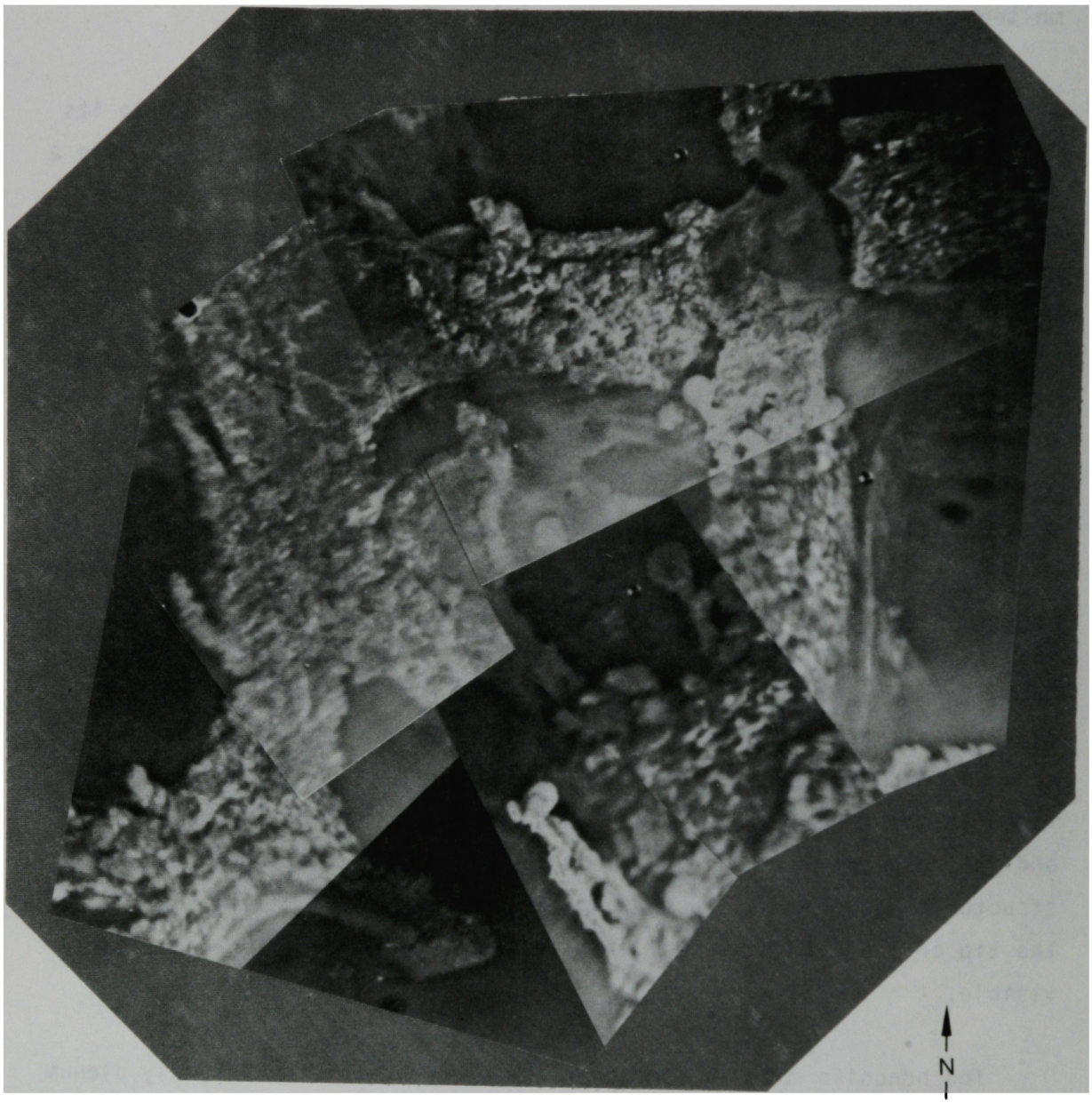

Figure 12. Damaged grid and guide structures over core position L10. Note the evidence of damage by foaming oxidation (irregular foamy appearance), melting (elongated frozen drops), and ablation (missing rib along south side), as well as the melting of guide structures above the grid.

Figure 13. Damaged grid structures over core position K9. While damage types are similar to those in Figure 12, the grid structures above the grid remain largely intact.

duration: it is difficult to visualize a situation where the nonuniformity in gas composition over a few centimeters across the flow path would not have averaged out over a long time. As seen in the heating calculations in Section 5, if the flow was maintained over a few minutes, the relatively thick grid pads and ribs would have melted along with the thin guide structures.

Multi-dimensional flow calculations have not been carried out to determine the upper plenum flow pattern. Thus, there has been no quantitative demonstration of the bifurcation of flow from the core to the upper plenum. However, based on the design of flow paths in the upper plenum, an explanation of the bifurcation may be offered. Figure 14 shows the azimuthal position of the main flow holes in the plenum cylinder superposed on the damage pattern in the underside of the upper grid. Instead of directly exiting the outlet nozzles, most of the flow from the core would rise from the core toward the large flow holes. It then would flow downward and around the outside of the plenum cylinder toward the outlet nozzles. One reason for such a flow path is the persistence of vertical momentum of the flow, making sharp turns toward the nozzles at lower elevations difficult. Another reason is that these flow holes are much larger than the ones at the nozzles, so they can carry more flow. Flow area differences also exist in the main flow holes themselves. There are three 34-inch flow holes in each half of the plenum cylinder situated toward the north and south quadrants, flanked by two 22-inch holes. In the east and west quadrants, no flow holes exist at the same elevation. The asymmetry in the design of the positions of the flow holes may have created two preferential directions of flow toward the north and south quadrants of the upper plenum. During normal operation, the fuel assemblies provide resistance to lateral flow, so the flow to the upper plenum is mostly vertical at the core exit and the flow diversion to the periphery occurs at higher elevations. During the accident, the central fuel assemblies collapsed to form a void in the upper core and, thus, the resistance to lateral flow was removed. It is likely that flow from the center of the core could have split into two streams below the upper grid toward the damaged areas.

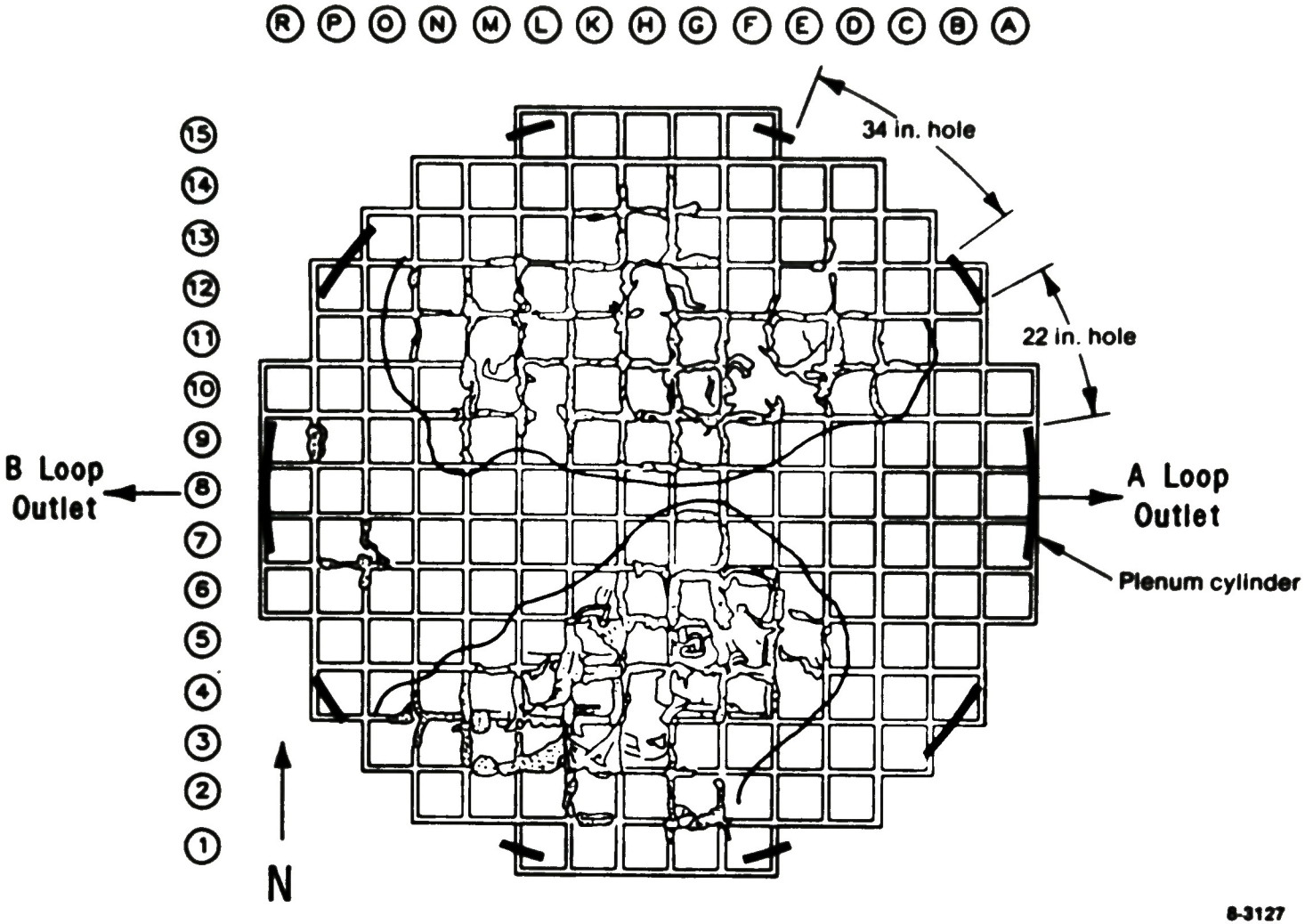

Figure 14. Azimuthal locations of main flow holes in the plenum cylinder in relation to plenum assembly damage pattern.

As mentioned earlier, the inhomogeneity in damage and the melting of only the relatively thin structures suggest a damage mechanism of short duration. Natural circulation is expected to last a relatively longer period of time. Once a circulation loop is set up, it will continue to circulate unless the heat source or the heat sink is removed. During the accident, the most likely period of natural circulation was between 110 min (core uncovery) and 174 min (2-B coolant pump restarted). The core probably attained high temperatures that could lead to significant plenum assembly heating around 140 min. The timescale of natural circulation would have been on the order of tens of minutes, much too long to adequately explain the characteristics of the observed damage.

Several sudden thermal-hydraulic disturbances in the primary coolant system were observed during the accident.[9] One was the 2-B primary coolant pump transient starting at 174 min into the accident, with a steep rise in system pressure over a couple of minutes. Another was at 224 min, also with a steep rise in system pressure, generally attributed to a rapid relocation of core material to the core bypass and the lower plenum. Between 15 and 16 hrs, attempts were made to start the primary coolant pumps. Sudden pressure drops were associated with these late pump starts. Except for the transient at 174 min, it is believed that the upper plenum was filled with cooling water prior to the other short transients. So it is unlikely that the plenum assembly could have been damaged during these other short transients, and the 2-B coolant pump transient starting at 174 min (precisely, 174 min 9 s after turbine trip) is left as the only short transient which could have caused the plenum assembly damage.

At the time of the pump transient, much of the reactor core was damaged. The hypothesized configuration consists of a bowl-shaped crust in the lower half of the core which contained partially melted core material. The crust was formed from a molten eutectic of uranium dioxide and zircaloy which had dripped from the top region of the core to near the water level in the lower region of the core. Fuel rod remnants remained in the upper core region. As the pump was restarted, a large amount of

water in the B-loop was delivered through the core, quenching the still intact rods of the peripheral assemblies to produce a copious amount of steam and driving up the system pressure.

The interaction between the water delivered by the 2-B coolant pump and the rod remnants in the upper part of the core is uncertain. The end state of the damaged configuration shows a rubblized particle bed collapsed onto the top of the consolidated region. The sudden pressure increase and thermal stress imposed on the rod remnants during the pump transient would have led to the formation of the rubble bed. However, it is unclear to what extent the rod remnants were quenched or the amount of hydrogen that could have been produced from the oxidation of the remaining zircaloy. If, during the pump transient, a mixture of high temperature steam and hydrogen was momentarily generated from the interaction of the incoming water and the rod remnants, and this mixture flowed to the upper plenum toward the large flow holes in the plenum cylinder, heat transfer from the mixture to the plenum assembly could provide a basis to explain the damage pattern and the damage characteristics observed in the upper plenum. The violent and transitory gas flow through the upper plenum could explain the inhomogeneity of the flow, and the presence of hydrogen in the gas mixture could explain the absence of oxidation in some of the damaged structures. The rapid oxidation of zircaloy, which generates intense heat, could also explain the localized presence of melted uranium dioxide in the rubble bed.

The calculations presented in the next two sections are based on the scenario that the plenum assembly was damaged during the 2-B pump transient. Section 4 (thermal-hydraulic calculations) shows that the amount of energy transferred to the fluid during the pump transient requires that the upper core rod remnants not be quenched, and that instead, hydrogen be produced from the unoxidized zircaloy. Section 5 (plenum assembly heating calculations) shows the importance of the presence of hydrogen in the hot gas stream such that extensive melting of the plenum assembly did not occur during a relatively short time period of the pump transient.

4. THERMAL-HYDRAULICS DURING THE 2-B COOLANT PUMP TRANSIENT

In terms of thermal-hydraulics, the TMI-2 accident was a small-break loss-of-coolant accident with coolant loss through the stuck-open pilot-operated relief valve (PORV) on top of the pressurizer. For the first 73 min of the accident, the reactor coolant pumps delivered a two-phase mixture of steam and water to the reactor core, keeping it from overheating. Due to excessive vibrations, the coolant pumps were successively stopped; first the B-loop pumps at 73 min, and then the A-loop pumps around 100 min. The stuck-open PORV was isolated at 139 min. After observing that core cooling was ineffective from natural circulation, attempts were made to restart the pumps around 170 min to force coolant through the core. At 174 min, the 2-B coolant pump was started successfully. The amount of water delivered to the core is indeterminate, but the effect of the running pump was to increase both the pressure of the primary system and that of the secondary side of the B-loop steam generator, indicating that heat was transferred from the reactor core to the primary fluid and to the fluid in the secondary side of the B steam generator. (No discernible effect was observed in the secondary side of the A steam generator.) The following subsections present analyses of such heat transfer. As a result of the analyses, steam generation rates from the reactor core are deduced. Assuming that all the generated steam flowed past the damaged zones in the plenum assembly, calculations on plenum assembly heating can be performed. Such calculations are documented in Section 5.

4.1 Heat Transfer to the B Steam Generator

Two measurements made in the B steam generator can be used to estimate the enthalpy gain in the fluid during the 2-B coolant pump transient. One is the liquid level measurement; the other, pressure measurement. These are gross measurements and, as such, do not yield any spatial distribution of mass and energy. Consequently, additional assumptions are required to estimate the enthalpy content of the fluid in

the steam generator. The simplest assumption required is that the fluid be divided into steam and liquid spaces, both at the saturation temperature corresponding to the measured pressure. The liquid level measurement gives the liquid volume. The remaining volume in the steam generator and the connecting steam line gives the steam volume. The pressure measurement and the assumption of saturation directly lead to the mass and the enthalpy content in the steam generator.

There had been little indication of sudden changes in the steam generator for quite some time before the 2-8 pump transient, so the assumption of saturation just before the pump transient should be quite satisfactory. However, during the pump transient, the pressure in the steam generator rose drastically due to the sudden vaporization of the liquid in the riser section of the steam generator. The timescale of the change was on the order of half a minute. Due to lack of heat transfer, the liquid in the downcomer section of the steam generator may have remained at the temperature corresponding to the saturation temperature just before the transient. As the pressure rose, the liquid in the downcomer would have been progressively subcooled, while the liquid in the riser would have been saturated.

The level measurement in the steam generator is schematically shown in Figure 15.[10] The measuring instrument was a differential pressure cell, registering the pressure difference between two elevations in the downcomer of the steam generator; one pressure tap was placed at the 2.59-m elevation above the bottom tube sheet, and the other at 7.42 m above the lower tap. The output of the instrument was actually a percentage of the full height between the pressure taps. To convert the pressure measurement to a percentage height, the following mathematical equivalent was built into the output circuit of the instrument:

$$\ell = \frac{100\ \Delta p}{\rho_{fd} g\ H_{op}}$$

where ℓ is the output level in percent of full height, H_{op}; Δp the differential pressure; ρ_{fd} the liquid density in the downcomer; and g the gravitational acceleration, all in SI units. The density was determined from temperature measurements in the downcomer. Based on this

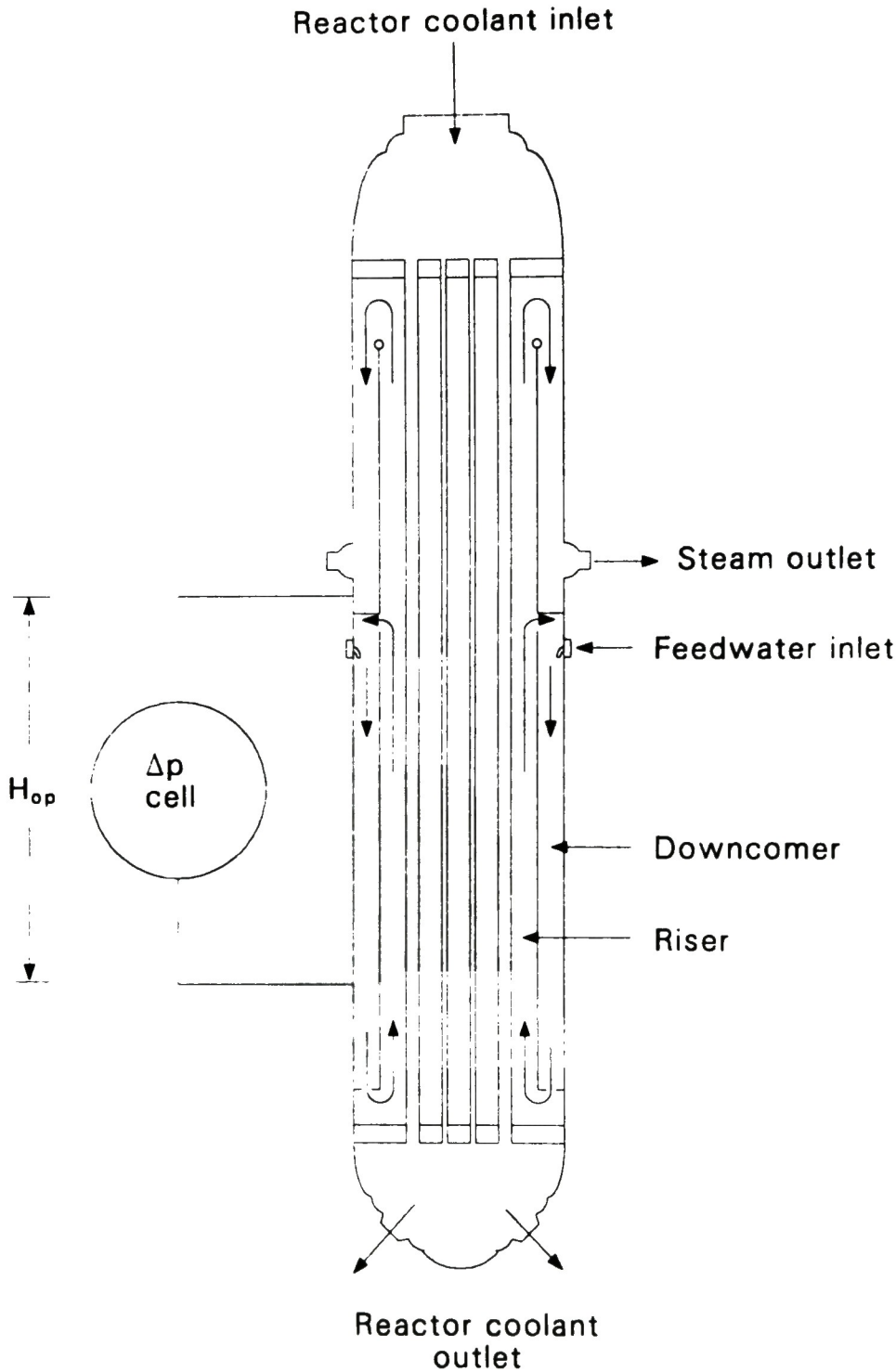

P556-WHT-288-06

Figure 15. Steam generator showing position of level measurement in the downcomer.

formulation, it is clear that the level (ℓH_{op}) indication was one of collapsed liquid level in the downcomer if all the steam between the pressure taps was condensed.

To obtain the true liquid level in either the downcomer or the riser section of the steam generator, assuming that the liquid and the steam were separated and stratified, the following equations are used:

$$\Delta p/g = 0.01\ \rho_{fd}\ \ell H_{op}$$

$$= \rho_{fr} L_r + \rho_g (H_{op} - L_r)$$

$$= \rho_{fd} L_d + \rho_g (H_{op} - L_d)$$

where L_r and L_d are the true liquid levels above the lower tap of the differential pressure measuring instrument in the riser and the downcomer, respectively; ρ_{fr} and ρ_{fd} the liquid densities in the riser and the downcomer, respectively; and ρ_g the steam density, assumed to be at saturation. Knowing the downcomer and the riser cross-section flow areas (2.167 m^2 and 3.946 m^2, respectively) and the total fluid volume of the steam generator and the connecting steam line (157.51 m^3),[10] the above equations are used to calculate the liquid and the steam masses.

From the liquid and the steam mass, it is straightforward to calculate the enthalpy content in the steam generator with the assumption that, before the transient, the system was at saturation, and after the initiation of the transient, only the liquid in the riser and the steam were at saturation, while the liquid in the downcomer remained at the pre-transient temperature. To obtain the enthalpy gain by the secondary from the primary, corrections have to be made to account for the inflow of auxiliary feedwater and the outflow of steam through the turbine bypass valve. For the results presented below, the auxiliary feedwater flow is set at 9.698 kg/s (cold water at an enthalpy of 1.6×10^5 J/kg). The steam outflow from the system between two times is calculated from the difference between the current mass and the sum of the mass at the beginning

of the time step and the inflow during the time step. The enthalpy lost from the system due to steam loss is assumed to have been supplied by the primary system.

The results of the analyses are presented in graphic form in Figures 16 through 19. The time origin in these plots corresponds to 174 min 9 s after turbine trip (nominal start time of the accident). This is the time when the 2-B coolant pump was successfully started. Figure 16 is the recorded pressure history during the transient, converted to SI units. Figure 17 is a comparison of the measured liquid level in the downcomer and the computed liquid level in the riser section of the steam generator. Note that the measured level shows a decrease immediately after time zero, while the computed level in the riser shows an increase. The decrease in the measured level can be understood by examining Figure 18, which shows a liquid mass decrease and a corresponding vapor mass increase during the same time period. Since the measurement represented roughly the liquid level in the downcomer where the liquid density did not change much, a decrease in the liquid inventory would show up as a level decrease. On the other hand, the riser section was heated to higher saturation temperatures as the pressure increased. The decrease in density of the liquid in the riser contributed to a net rise in the liquid level despite a depletion in liquid inventory. The energy transfer to the secondary side of the steam generator (enthalpy gain) from the primary side is shown in Figure 19. This will be combined with the enthalpy gain by the primary fluid, analyzed in the next section, to give the total energy transfer from the reactor core during the pump transient.

4.2 Thermal-Hydraulics of the Primary System Fluid

Heat transfer to the primary coolant system during the 2-B coolant pump transient is obtained by calculating the enthalpy content of the primary fluid as a function of time. No attempt is made to model the primary system in detail; this may be left to a future calculation using a sophisticated code like SCDAP/RELAP5.[11] However, estimates of the enthalpy content of the primary system fluid can be made with the aid of a

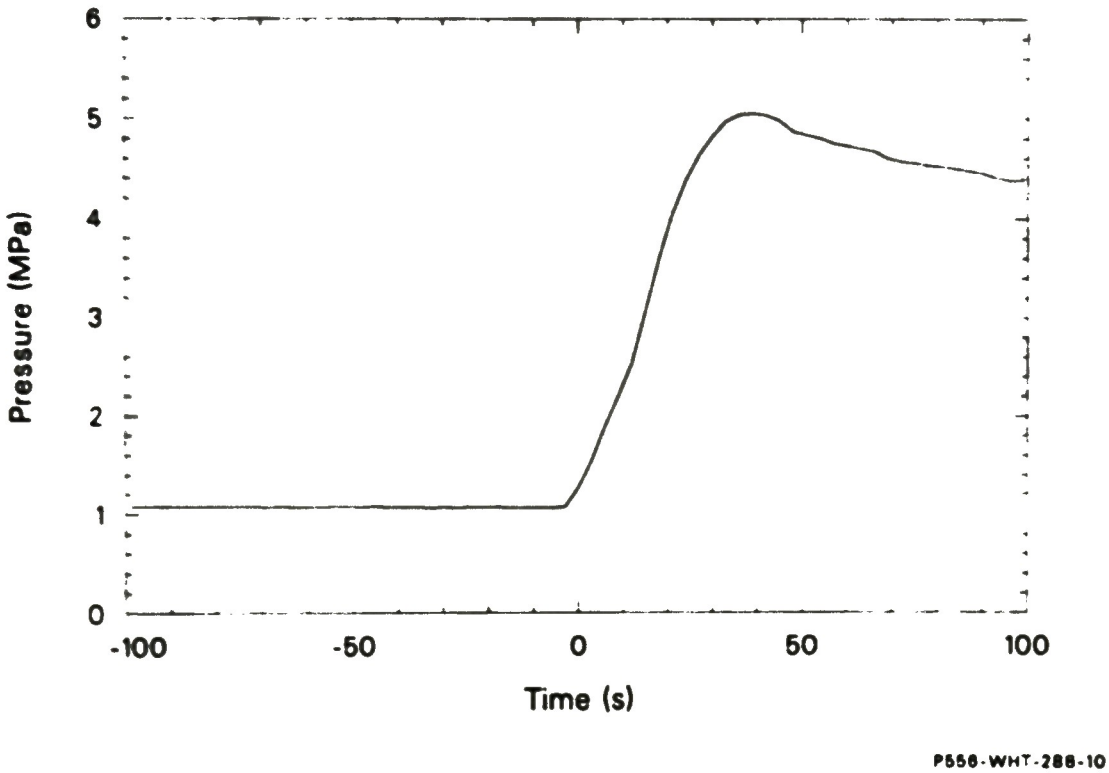

Figure 16. Steam generator B secondary side pressure during the 2-B pump transient. (Time o = 174 min 9 s after turbine trip)

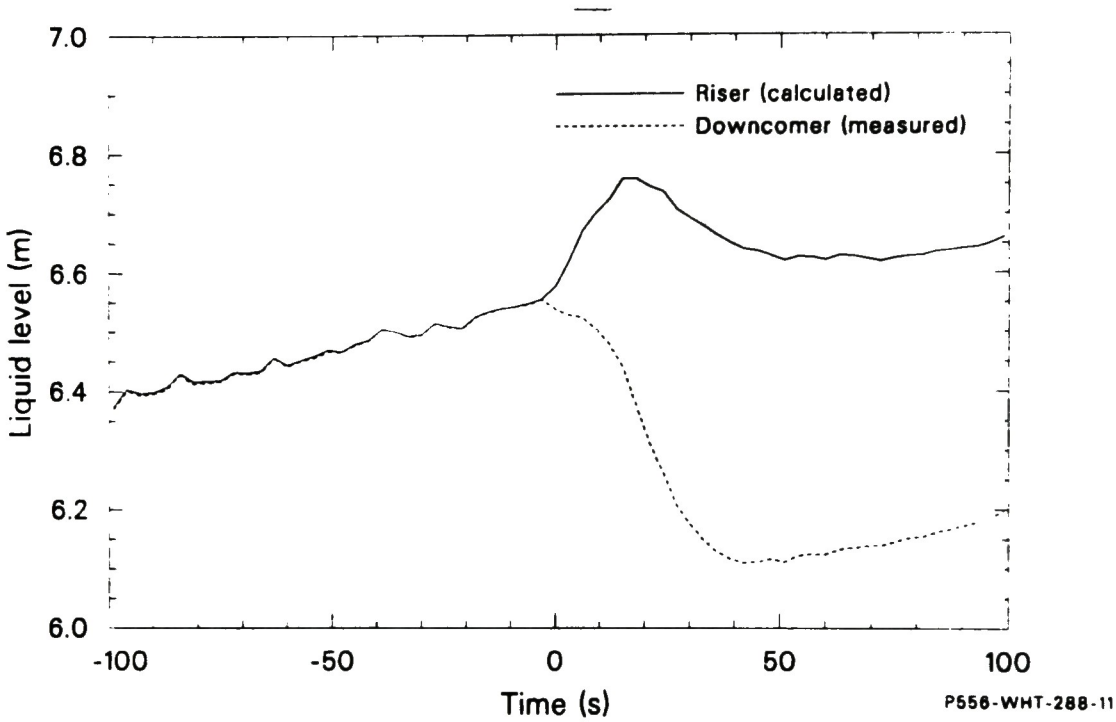

Figure 17. Steam generator B riser secondary side liquid level and measured downcomer liquid level during the 2-B pump transient. (Time o = 174 min 9 s after turbine trip)

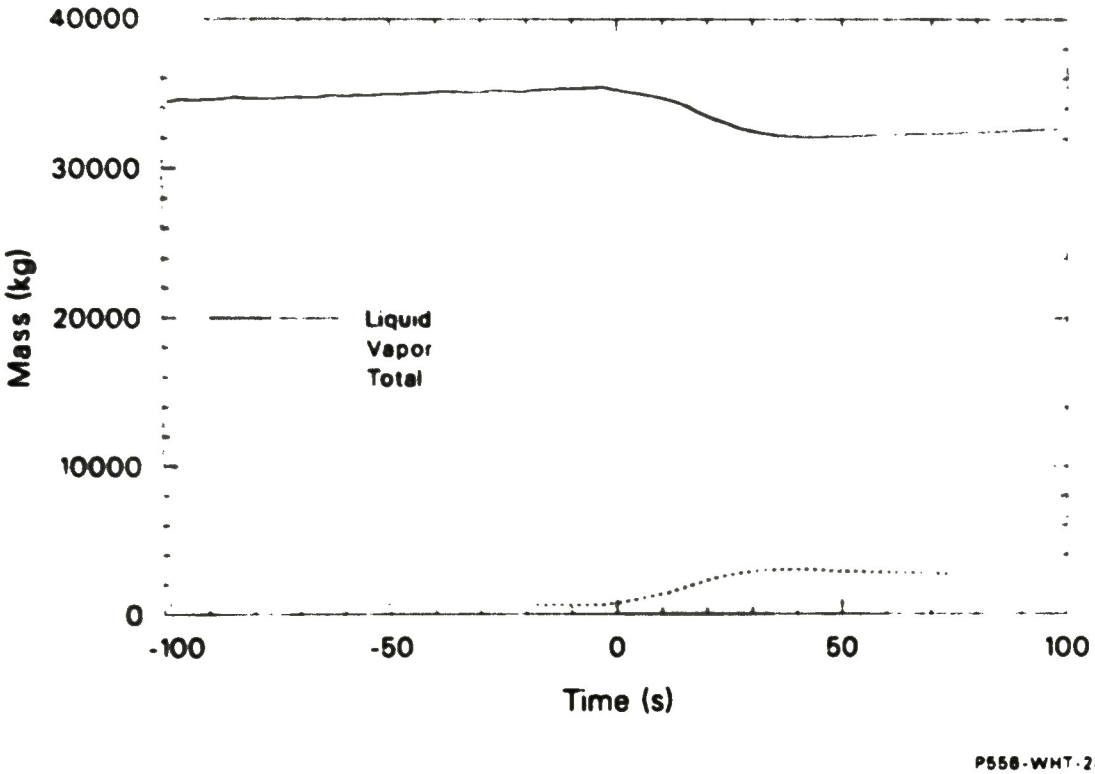

Figure 18. Mass partition between vapor and liquid on secondary side of B steam generator during the 2-B pump transient. (Time 0 = 174 min 9 s after turbine trip)

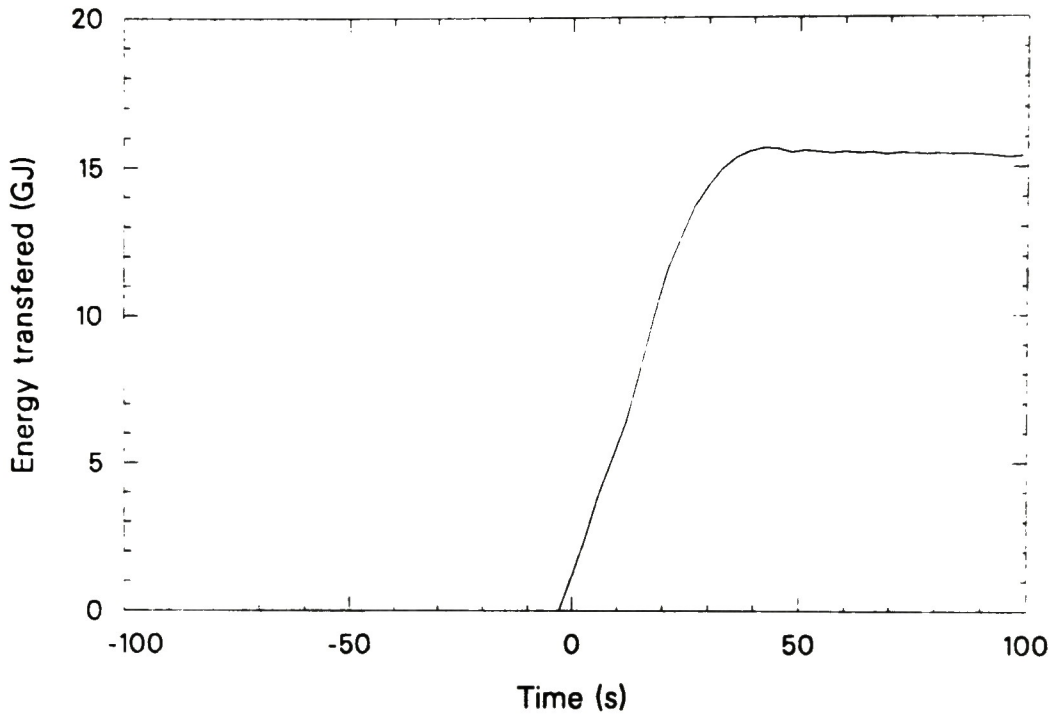

Figure 19. Cumulative energy transfer to the B steam generator secondary side during the 2-B pump transient. (Time o = 174 min 9 s after turbine trip)

few simple assumptions. These assumptions are discussed below, followed by the equations governing the partition of liquid and vapor volumes in the primary system and the solutions of the equations. The masses of liquid and vapor, as well as the enthalpy of the system, can be derived directly from these solutions. The results are again presented in graphic form at the end of the section.

At the time of the pump transient, the PORV was isolated, and for the short duration of the pump transient, makeup and letdown flows were negligible compared to the total system mass. Thus, the fluid mass in the system can be assumed constant without introducing much error. Most of the error would come from the determination of the value of the constant. Another assumption that is required is the state of the fluid. For the liquid, it is assumed that it is at the saturation temperature corresponding to the recorded system pressure. For the vapor, it is assumed that that portion occupying part of the reactor core and the reactor vessel upper plenum was at high temperature, while the rest was at the saturation temperature. These assumptions lead to the following equations:

$$V_h + V_s = V_g$$

$$V_g + V_l = V$$

$$\rho_h V_h + \rho_s V_s + \rho_l V_l = M ,$$

where the V's are the volumes, ρ's the densities, and M the total fluid mass in the system. The subscript, h, refers to hot vapor, s, saturated vapor, g, total vapor, and l, liquid. The solutions of the equations are given by

$$V_l = \frac{M + V_h (\rho_s - \rho_h) - \rho_s V}{\rho_l - \rho_s}$$

$$V_g = \frac{\rho_l V - M - V_h (\rho_s - \rho_h)}{\rho_l - \rho_s} .$$

The values of V, V_h, and M are presumed known. For a given pressure, the densities at saturation can be obtained from a steam table. The hot vapor density depends on the assumed high temperature. For the subsequent analysis, it is assigned a value of 1500 K. Besides the somewhat arbitrariness of this high temperature, the determination of the gas density is complicated by the presence of hydrogen in the system, released from the oxidation of zirconium by steam. Fortunately, since one mole of steam consumed in the oxidation of zirconium yields one mole of hydrogen, the volume occupied by the hydrogen at high temperatures differs little from the volume of the steam from which it is converted. In the calculations, it can therefore be assumed that all the gas was steam without introducing much error in the determination of the liquid and gas volumes. This assumption also makes the system fluid mass precisely constant in the absence of inflows and outflows.

To assign a value to the mass of the fluid in the primary system, knowledge of the primary system volume distribution is required. This is shown in Figure 20. From the sequence of events and an accident scenario, the fluid mass in the primary system is estimated as follows. Just before the pump transient, most of the reactor core must have been voided to explain the final damage state of the reactor core. To equalize the hydrostatic head in the core, the liquid level in the downcomer of the reactor vessel must also have been fairly low. If there was any water left in the core and the downcomer, the lower plenum of the reactor vessel would also be filled with water. Because the B-loop reactor coolant pumps were turned off quite early in the accident (73 min), the liquid in the B-loop would have filled up to the level of the pump discharge. Any excess water would have drained to the core. The A-loop coolant pumps were turned off late (100 min) when the void fraction in the system had reached a higher level due to the continual loss of fluid through the PORV and the letdown system. The liquid probably only filled one-half of the volume of the A-loop below the level of the pump discharge. Level measurement in the pressurizer was recorded and just before the pump transient, the measurement indicates that the pressurizer was about half full. With this discussion of the likely liquid volume in the system, and assuming that the

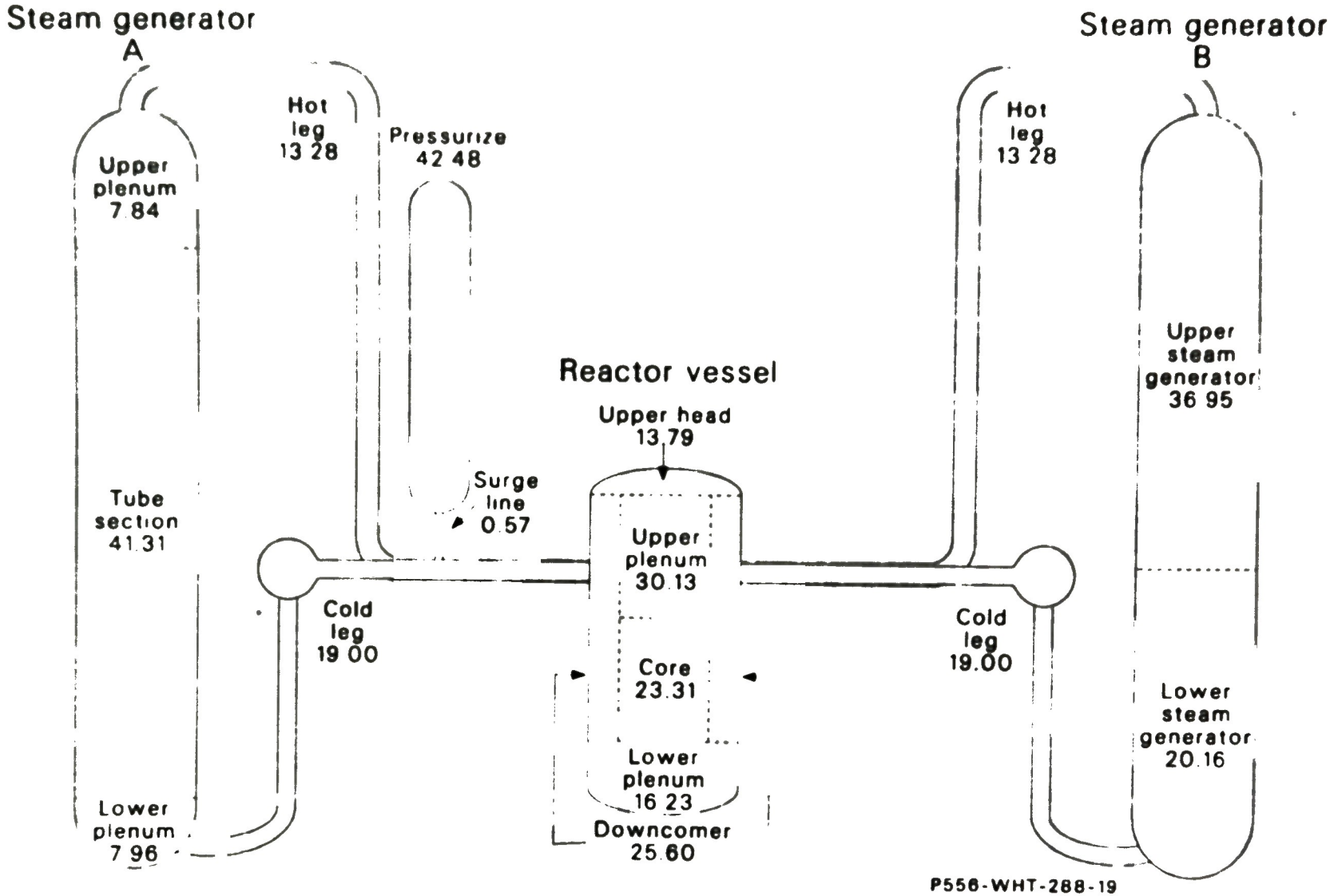

Figure 20. Primary cooling system volume distribution. Volumes are in m^3.

remaining space in the primary system was filled with steam, the total system fluid mass would have been between 80,000 and 90,000 kg. This is consistent with a mass of 85,000 kg obtained in a recent trial calculation using SCDAP/RELAP5.[12]

To estimate the volume of the hot gas in the system, the volume distribution shown in Figure 20 again is used. If two-thirds of the core and most of the upper plenum were at high temperature, the volume of the hot gas would have been about 42 m^3.

Based on the above discussions, the parameters used in the simplified thermal-hydraulic calculations are summarized in Table 2. These parameters and the measured system pressure used in conjunction with the equations presented in this section are sufficient for the calculation of the fluid enthalpy in the primary system and the partition of the mass into liquid water and steam.

The measured primary system pressure is shown in Figure 21. The partition of the fluid mass into liquid and steam is shown in Figure 22. The increase in steam mass indicates net vaporization in the primary system. The enthalpy of the primary system fluid over its value at the beginning of the pump transient is shown in Figure 23. The time origin in all plots again corresponds to the time when the 2-B coolant pump was started (174 min 9 s after turbine trip).

4.3 Hot Gas Generation in the Reactor Core

The net steam generation during the 2-B coolant pump transient is given in the last section (derivable from Figure 22). To obtain the total steam flow out of the reactor core, the amount of condensed vapor in the primary side of the B steam generator has to be added to the net steam generation. The amount of heat gain by the secondary side of the B steam generator (Figure 19) must correspond to an equal amount of heat loss in the primary side of the steam generator. In assuming that the fluid was at saturation in the steam generator in the primary side, such heat loss must

TABLE 2. PRIMARY COOLING SYSTEM FLUID PARAMETERS

Total volume	331 m^3
Total mass	85,000 kg
Hot gas volume	42 m^3
Hot gas temperature	1,500 K
Volume at saturation	289 m^3

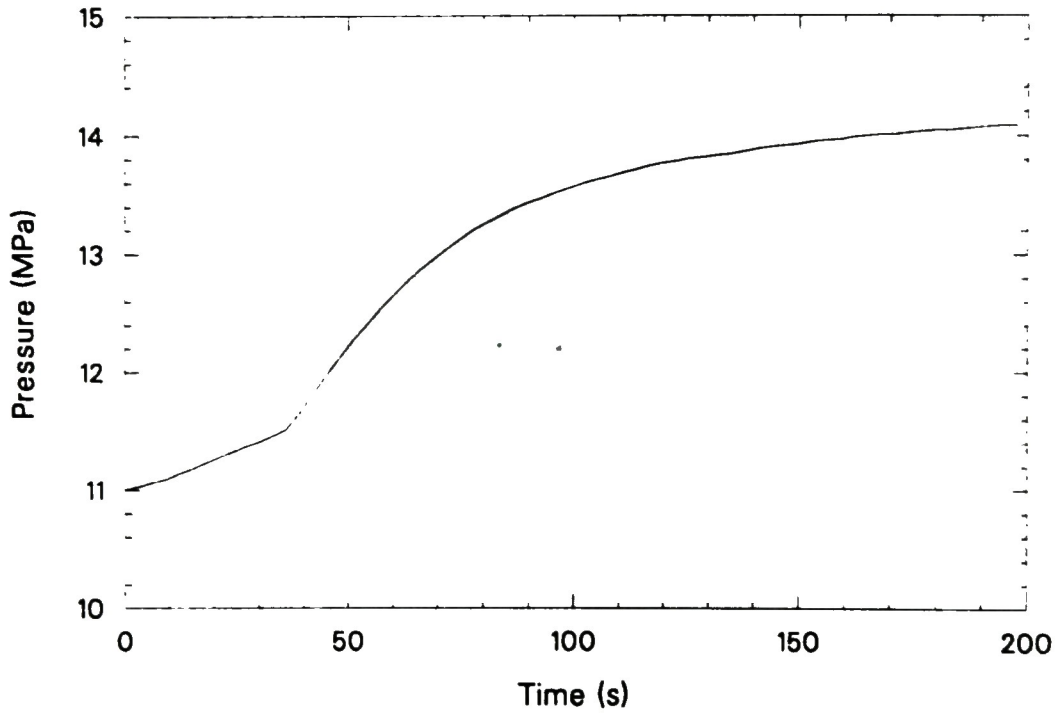

Figure 21. Primary system pressure during the 2-B pump transient. (Time o = 174 min 9 s after turbine trip)

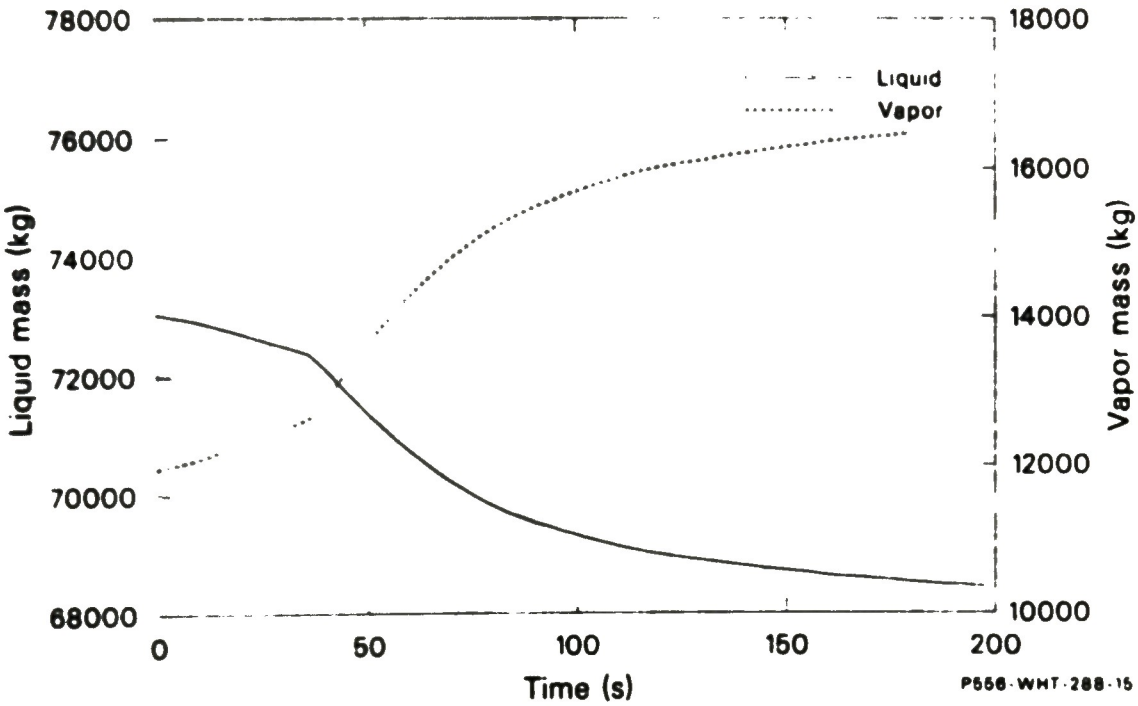

Figure 22. Primary system mass partition between vapor and liquid during the 2-B pump transient. (Time 0 = 174 min 9 s after turbine trip)

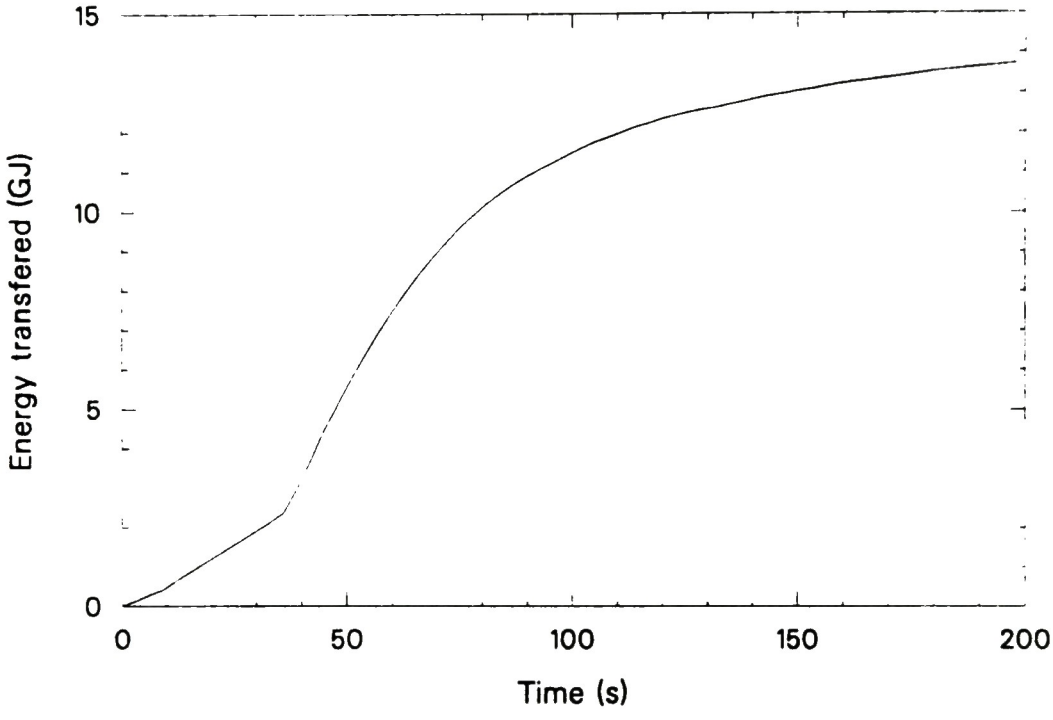

Figure 23. Net energy transferred to the primary system fluid during the 2-B pump transient. (Time o = 174 min 9 s after turbine trip)

have come from condensation of the saturated steam. Therefore, the amount of condensation is simply the heat gain by the secondary side of the steam generator divided by the latent heat of vaporization. The total steam generation rate from the reactor core obtained from such calculations is shown in Figure 24.

The total energy transfer from the reactor core is of interest in arriving at an estimate of hydrogen generation during the pump transient. The total energy transfer is the sum of the enthalpy transferred to and retained by the primary system fluid, and the enthalpy gain by the secondary system fluid. Combining the results given in Figures 20 and 23, the total energy transfer is shown in Figure 25 and the rate of energy transfer in Figure 26. Because of the short duration of the pump transient, decay heat can be ignored. The main source of heat was a combination of the heat stored in the core material and the heat generated in the oxidation of zirconium. From Figure 25, the total energy transfer was about 3×10^{10} J. The total heat flux during quench of the debris bed on top of the consolidated region is estimated to be less than 4 MW, or a total heat flow less than 8×10^{8} J over a 200-second period--an insignificant fraction of the total energy transfer.[13] Because of its large size (about 1 m in its smallest dimension), the consolidated region also would not have contributed much heat to the fluid. If the peripheral assemblies (25,000 kg) were quenched from 1200 K, they could have provided 6×10^{9} J, leaving 2.4×10^{10} J to come from oxidation. This was equivalent to the oxidation of 3700 kg of zirconium, about 16% of the zirconium inventory in the core, and the generation of 160 kg of hydrogen (80,000 gram-moles). The net gas generation in the primary system (total minus condensation) was equivalent to 4600 kg of steam, or 250,000 gram-moles. So an appreciable fraction (~32% molar) of the uncondensed gas generated during the pump transient must have been hydrogen.

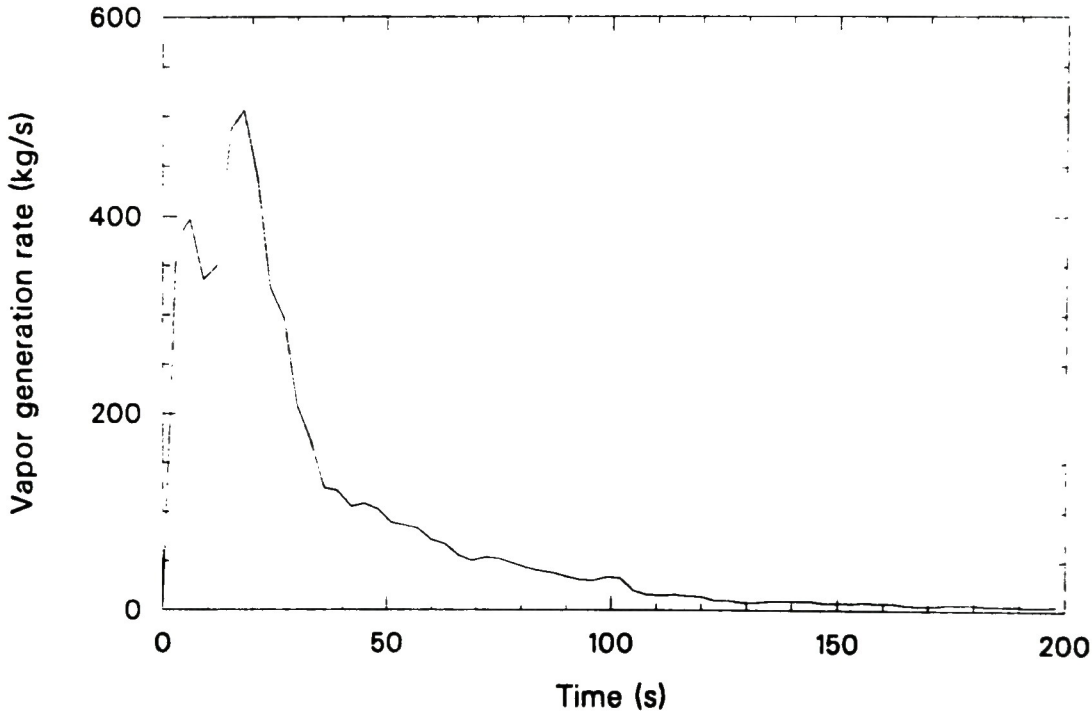

Figure 24. Steam generation rate in the reactor core during the 2-B pump transient. (Time o = 174 min 9 s after turbine trip)

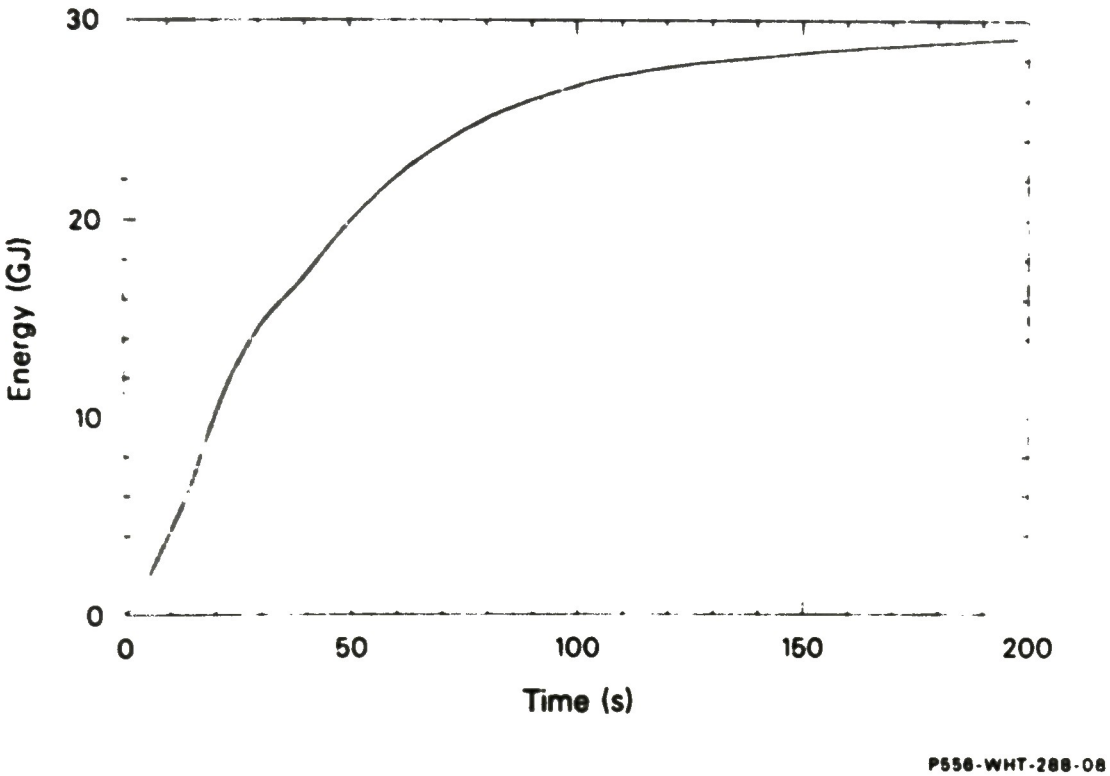

Figure 25. Total energy transfer from the reactor core to the reactor cooling system during the 2-B pump transient. (Time o = 174 min 9 s after turbine trip)

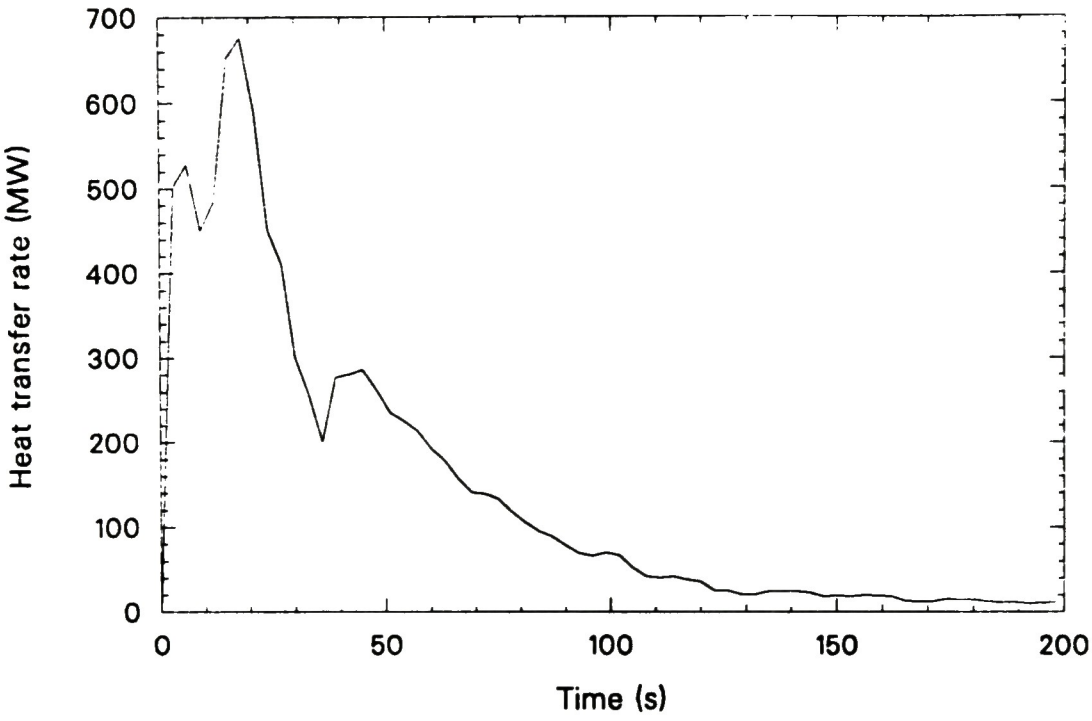

Figure 26. Heat transfer rate from the reactor core to the reactor cooling system during the 2-B pump transient. (Time o = 174 min 9 s after turbine trip)

5. PLENUM ASSEMBLY HEATING CALCULATIONS

The groundwork for plenum assembly heating calculations during the 2-8 primary coolant pump transient has been laid in the previous sections. Section 2 outlines the design geometry of the upper plenum from which a calculational model can be constructed. The observed damage in the plenum assembly, as described in Section 3, leads to a conjecture that most of the hot gas flow during the transient was directed toward the damaged regions. Section 4 analyzes the thermal-hydraulics to yield the mass flow rate from the core during the pump transient and the results of the analysis also indicate that an appreciable amount of hydrogen must have been produced during the transient to explain the total energy transfer to the primary and the secondary fluid. This section is organized to give a description of the model geometry (Section 5.1), the heat transfer correlations and parameters (Section 5.2), and the results of the calculations (Section 5.3). Particular emphasis is placed on the degree of melting of the plenum assembly structures as a result of the hot gas flow through the upper plenum during the pump transient.

5.1 Model Geometry

In regions of observed damage in the plenum assembly, away from the periphery of the assembly, the geometry is one of repeated patterns of a grid position with a control rod guide assembly, alternating with a grid position without such a structure. Therefore, a unit cell of the plenum grid structure away from its periphery consists of two adjacent positions, one with a control rod guide assembly, the other without. In the heating calculations, only one such unit cell is considered.

The thermal calculation model of a unit cell of the plenum assembly is shown in Figure 27. The figure identifies the components modeled in the heat transfer calculations but does not represent the actual arrangement of the components, except for their relative elevations. All the structures are modeled up to the 0.489-m elevation, relative to the bottom of the upper end fittings of the fuel assemblies. These include the end fittings,

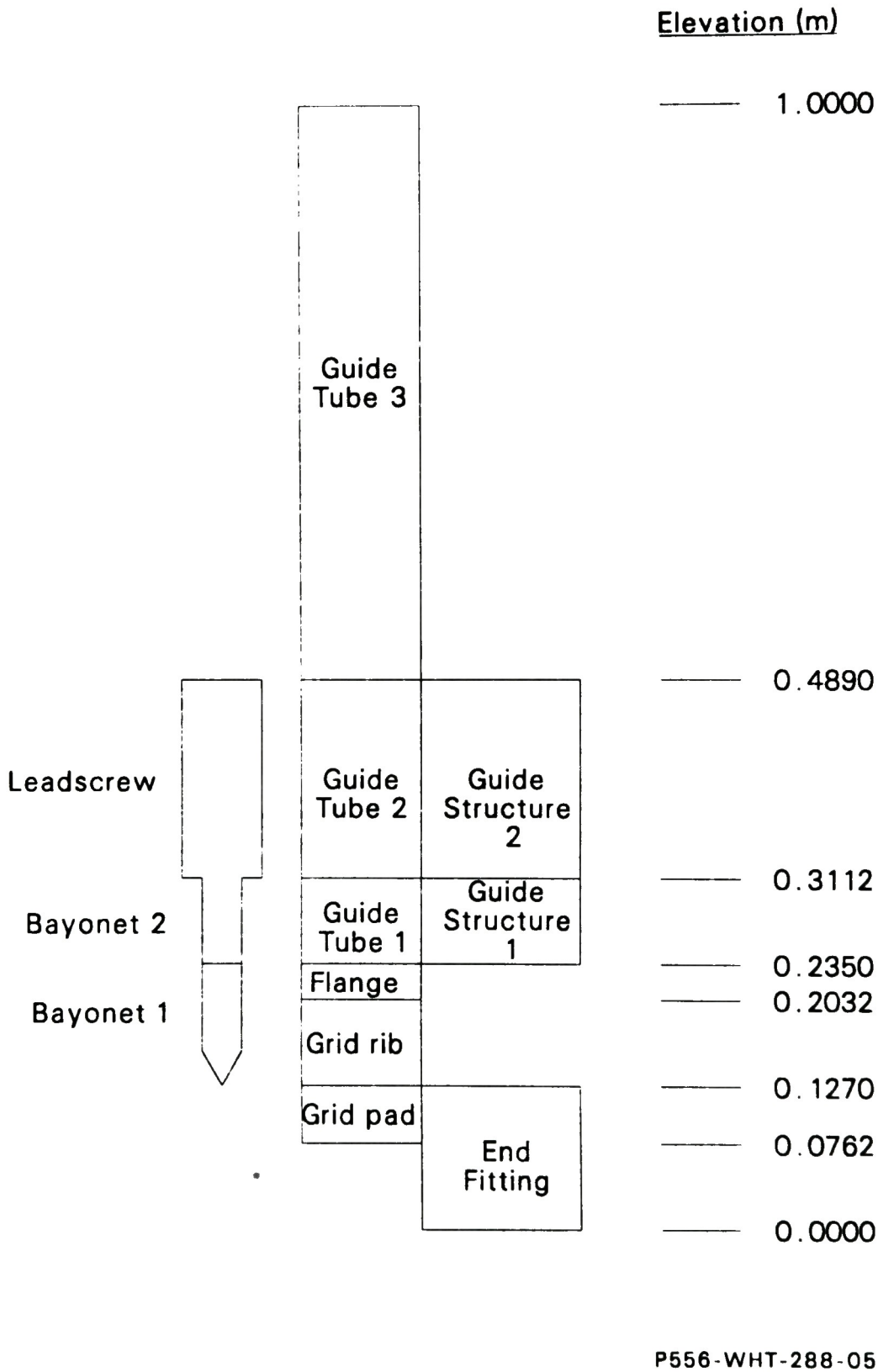

Figure 27. Model of a plenum assembly grid structure unit cell for thermal calculations.

grid pads, grid ribs, flange of the control rod guide assembly tubular housing (hereafter called the "guide tube"), the guide tube itself, the fine structures inside the guide tube (split and "C" tubes and cast support plates), bayonet tip of the leadscrew, and the leadscrew above the bayonet. Above the 0.489-m level, only the guide tube is modeled. Omission of the other structures is justified on the grounds that any hot gas entering the interior of the guide tube from the core would have exited through the holes in the lower part of the guide tube once it reached the 0.489-m elevation. Consequently, the structures interior to the guide tube would not be heated directly by the hot gas above this elevation and heat transfer to them could be ignored. The model is terminated at the 1.0-m elevation, so the plenum cover structures are omitted in the model. As the results of the calculations would indicate, this is sufficient to estimate the amount of melted material in the plenum assembly during the pump transient.

A lumped parameter approach is used in the heat transfer calculations. The structures are divided into vertical zones, ten per structure. Each structure is characterized by two parameters: the mass per unit length and the surface area per unit mass; or its equivalent, surface area per unit length. Heat gain by a structure is uniformly distributed in each zone, so there is only one temperature characterizing a zone of a structure. The vertical temperature distribution, however, depends on the amount of heat transferred to the various zones. Heat conduction between zones is ignored, as is the radiation exchange. The parameters characterizing the structures are given in Table 3. The mass of the end fitting is obtained by weighing an end fitting similar to the ones used in the TMI-2 reactor. The surface area of an end fitting is estimated from the average thickness of its inner structures. Parameters of the other structures listed in Table 3 are all derived from the information presented in Section 2. Because all the structures have about the same density and specific heat (with the exception of the end fittings, which contain some Inconel, all the other structures are made of stainless steel), the ratio of the surface area per unit length to the mass per unit length is a measure of the surface area to heat capacity ratio. For a given heat flux

TABLE 3. PLENUM ASSEMBLY STRUCTURE PARAMETERS FOR A UNIT CELL

Structure Description	Mass per unit length M_1 (kg/m)	Surface area per unit length A_1 (m)	A_1/M_1 (m^2/kg)
Upper end fitting	242.0	23.80	9.83 E-2
Grid pad	135.9	1.36	1.00 E-2
Grid rib and flange	181.1	1.43	7.90 E-3
Bayonet	2.3	0.06	2.61 E-2
Guide structure	12.2	1.22	1.00 E-1
Leadscrew	9.1	0.12	1.32 E-2
Lower guide tube	29.4	0.93	3.16 E-2
Upper guide tube	42.2	0.69	1.64 E-2

transferred to the structures, the higher this ratio is, the faster the rise in the structure's temperature. For example, the upper end fittings and the guide structures inside the guide tubes (highest surface area to mass ratio) are the easiest to heat, while the grid pads and the grid ribs (lowest surface area to mass ratio) are the most difficult to heat. This thermal behavior is confirmed by the calculations.

5.2 Heat Transfer Correlations and Parameters

Convective and radiative heat transfer from the hot gas to the plenum assembly structures are considered. Hot gas flow through the upper plenum is assumed to be one-dimensional and in the vertical direction. All the hot gas generated in the core during the pump transient is assumed to go through only those grid positions where damage has been observed, or for a total of 61 equivalent positions. For a unit cell, which consists of two grid positions, the flow rate is obtained by dividing the vapor generation rate (as shown in Figure 24) by 30.5. The temperature of the gas is assumed to be 2000 K, the maximum average temperature attained by the particles in the upper core debris bed.[2]

The convective heat transfer correlation used is one for laminar flow past a flat plate. The correlation[14] is given by

$$h_{conv} = 0.332 j.C_p.Pr^{-2/3}.(\mu/(j.x))^{1/2}$$

where h_{conv} is the heat transfer coefficient, j the mass flux, C_p the specific heat at constant pressure, Pr the Prandtl number, μ the dynamic viscosity, and x the distance from the leading edge of the plate. The distance is measured from the bottom of the end fitting at the beginning of the transient and from the elevation below which all the material has been calculated to be melted as the transient proceeds. The convective heat flux is given by the product of the heat transfer coefficient and the temperature difference between the gas and the structure.

The fluid properties used in the convective heat transfer coefficient are those for steam at high temperatures (about 1600 K). These are

$$C_p = 2700 \text{ J/kg-K}, \quad Pr = 0.9, \quad \text{and} \quad \mu = 6.3 \times 10^{-5} \text{ Pa-s}$$

and are taken to be constants in the calculations.

The mass flux j, depends on the mass flow rate and the flow area through the structures. For a unit cell below the 0.489-m elevation, it is assumed that the gas flows on both the inside and outside of the guide tube and the flow area is about 0.1 m^2. Above the 0.489-m elevation, it is assumed that the gas flows only on the outside of the guide tube and the flow area is about 0.06 m^2. With these parameters, the use of the laminar correlation is justified because during most of the transient, the Reynolds number based on a length scale measured from the leading edge is less than 4×10^5.

The radiative heat flux, q_{rad}, from the hot gas to the heat structures is given by

$$q_{rad} = \varepsilon . \sigma . (T^4 - T_w^4)$$

where ε is the effective emissivity of the gas, σ the Stefan-Boltzmann constant, T the absolute temperature of the gas, and T_w the absolute temperature of the structure. The emissivity depends on the composition and the dimension of the gas. In the temperature and pressure range of interest (1400 to 2000 K, 15 MPa, respectively), the steam emissivity for 1 m of path length is close to 0.7,[15] but the hydrogen emissivity is practically nil.[16] In the calculations, the emissivity is taken as a parameter between 0.3 and 0.7. The low end of the emissivity range is representative of a gas with an appreciable hydrogen content, and the high end--a gas which is mostly steam.

The total heat transfer to a structure is the sum of the convective and radiative heat flux multiplied by the surface area of the structure. The enthalpy rise, ΔH, in a structure is given by

$$\Delta H = [h_{conv} \cdot (T - T_w) + q_{rad}] \cdot A_l / M_l$$

where A_l and M_l are the surface area per unit length and the mass per unit length of the structures, respectively, as given in Table 3. The above formula is applicable to zones of structures which have not been melted. For a partial melting of a zone, assuming that the melted material moves away from the structure, the enthalpy rise is increased by a factor of $1/(1 - f)$, where f is the melted fraction. For a complete melt, the structure is left out in the calculations.

To convert enthalpy of the structures to a temperature, it is assumed that the specific heat of the material (steel or Inconel) is 530 J/kg-K; the material melts at 1750 K and its heat of fusion is 2.5×10^5 J/kg.

At any elevation, the total heat loss from the gas to all the structures is obtained by summing over the heat transfer at that elevation. The amount of heat loss is subtracted from the current enthalpy of the gas to obtain the enthalpy of the gas at the next higher elevation. The enthalpy of the gas is converted to a gas temperature in the heat transfer calculations.

As an initial condition for the structures, it is assumed that the temperature is 1000 K at the base of the end fittings and decreases linearly to 700 K at the 1-m elevation.

The above description provides all the necessary parameters for the heatup calculations. The calculations are terminated at 150 s after the initiation of the pump transient, after which time the hot gas flow to the upper plenum becomes negligible. The calculated melt distribution at 150 s in the upper plenum can be compared directly to the observed damage. The calculated temperature distribution may be used to compare with any future determinations of the maximum temperature attained by the structures during the accident.

5.3 Temperature and Melt Distributions

Plenum assembly heating calculations are performed for three values of the effective gas emissivity--0.3, 0.5 and 0.7. The results are presented in Tables 4 through 6. Listed in the tables are the structures (as depicted in Figure 27), their temperatures and melted fractions for three times after the initiation of the pump transient (174 min 9 s). At the bottom of each table, the total amount of melted material in the plenum assembly and total energy transferred to the structures are also given. The total amounts are for the 61 equivalent damaged grid positions.

For all three calculations, the tables show that the upper end fittings are melted within 30 s. This is consistent with the observation that almost all of the upper end fittings associated with damaged grids were missing at the end of the accident. (The locations of the missing upper end fittings are shown superposed on the damaged grid positions in Figure 11.) The end fittings could have fallen off when the fuel assemblies collapsed, instead of being melted away. However, the presence of other end fittings still attached to the upper grid prior to the partial lifting of the plenum assembly in December 1984, would indicate that at least some of the end fittings associated with the damaged grid positions must have stuck between the ribs and were later melted away.

The next structures to melt after the end fittings are the guide structures of the control rod guide assemblies. All three calculations indicate that those structures up to the 0.489-m elevation would have melted within 100 s. Above the 0.489-m elevation, it has been assumed that the hot gas flowed on the outside of the guide tube. Under such a condition, those structures above the 0.489-m elevation would have been shielded from the hot gas by the guide tube and would not have been heated to damaging temperatures.

At the end of 150 s, all three calculations show that the temperatures of the structures exceed 1700 K. With increasing emissivity and, hence, increasing radiative heat flux, the total amount of heat transferred to the structures is increased. For emissivity equal to 0.3,

TABLE 4. PLENUM ASSEMBLY HEATING FOR GAS EMISSIVITY = 0.3

Time	30 s		100 s		150 s	
Structure	Temp (K)	Melt Fraction	Temp (K)	Melt Fraction	Temp (K)	Melt Fraction
End fitting	--	1.00	--	1.00	--	1.00
Pad	1289.7	0.00	1689.4	0.05	1750.0	0.22
Rib + flange	1147.1	0.00	1481.9	0.00	1750.0	0.01
Bayonet 1	1514.3	0.00	1750.0	0.68	--	1.00
Bayonet 2	1416.5	0.00	1750.0	0.43	1750.0	0.95
Guides 1	1750.0	0.68	--	1.00	-	1.00
Guides 2	1750.0	0.52	--	1.00	--	1.00
Tube 1	1493.1	0.00	1750.0	0.71	--	1.00
Tube 2	1434.3	0.00	1750.0	0.58	--	1.00
Tube 3	1094.0	0.00	1601.5	0.01	1738.7	0.06
Leadscrew	1136.7	0.00	1552.3	0.00	1719.4	0.00
Melted material (kg)	991		1195		1364	
Energy transfer (GJ)	0.965		1.392		1.536	

Notes: Elevation of tall structures above bottom of end fitting:
Bayonet 1 - 0.127 to 0.235 m; Bayonet 2 - 0.235 to 0.311 m;
Guides - 0.235 to 0.311 m; Guides 2 - 0.311 to 0.489 m;
Tube 1 - 0.235 to 0.311 m; Tube 2 - 0.311 to 0.489 m;
Tube 3 - 0.489 to 1.0 m; Leadscrew - 0.311 to 0.489 m.

Melted material and energy transfer based on 61 grid positions.

TABLE 5. PLENUM ASSEMBLY HEATING FOR GAS EMISSIVITY = 0.5

Time	30 s		100 s		150 s	
Structure	Temp (K)	Melt Fraction	Temp (K)	Melt Fraction	Temp (K)	Melt Fraction
End fitting	--	1.00	--	1.00	--	1.00
Pad	1378.3	0.00	1750.0	0.22	1750.0	0.63
Rib + flange	1214.6	0.00	1630.6	0.01	1750.0	0.09
Bayonet 1	1650.6	0.01	--	1.00	--	1.00
Bayonet 2	1569.7	0.00	--	1.00	--	1.00
Guides 1	--	1.00	--	1.00	--	1.00
Guides 2	--	1.00	--	1.00	--	1.00
Tube 1	1655.9	0.00	--	1.00	--	1.00
Tube 2	1608.1	0.00	--	1.00	--	1.00
Tube 3	1221.0	0.00	1750.0	0.15	1750.0	0.58
Leadscrew	1236.0	0.00	1747.5	0.02	1750.0	0.42
Melted material (kg)	1032		1427		1861	
Energy transfer (GJ)	1.075		1.561		1.707	

Notes: Elevation of tall structures above bottom of end fitting:
Bayonet 1 - 0.127 to 0.235 m; Bayonet 2 - 0.235 to 0.311 m;
Guides - 0.235 to 0.311 m; Guides 2 - 0.311 to 0.489 m;
Tube 1 - 0.235 to 0.311 m; Tube 2 - 0.311 to 0.489 m;
Tube 3 - 0.489 to 1.0 m; Leadscrew - 0.311 to 0.489 m.

Melted material and energy transfer based on 61 grid positions.

TABLE 6. PLENUM ASSEMBLY HEATING FOR GAS EMISSIVITY = 0.7

Time	30 s		100 s		150 s	
Structure	Temp (K)	Melt Fraction	Temp (K)	Melt Fraction	Temp (K)	Melt Fraction
End fitting	--	1.00	--	1.00	--	1.00
Pad	1453.5	0.00	1750.0	0.51	1750.0	0.96
Rib + flange	1278.0	0.00	1737.5	0.04	1750.0	0.38
Bayonet 1	1742.4	0.05	--	1.00	--	1.00
Bayonet 2	1691.6	0.00	--	1.00	--	1.00
Guides 1	--	1.00	--	1.00	--	1.00
Guides 2	--	1.00	--	1.00	--	1.00
Tube 1	1750.0	0.06	--	1.00	--	1.00
Tube 2	1737.4	0.00	--	1.00	--	1.00
Tube 3	1340.2	0.00	1750.0	0.55	1750.0	0.98
Leadscrew	1328.5	0.00	1750.0	0.36	1750.0	0.88
Melted material (kg)	1037		1780		2394	
Energy transfer (GJ)	1.164		1.683		1.841	

Notes: Elevation of tall structures above bottom of end fitting:
Bayonet 1 - 0.127 to 0.235 m; Bayonet 2 - 0.235 to 0.311 m;
Guides - 0.235 to 0.311 m; Guides 2 - 0.311 to 0.489 m;
Tube 1 - 0.235 to 0.311 m; Tube 2 - 0.311 to 0.489 m;
Tube 3 - 0.489 to 1.0 m; Leadscrew - 0.311 to 0.489 m.

Melted material and energy transfer based on 61 grid positions.

the average fraction of radiative heat flux is 68% of the total heat flux; for emissivity equal to 0.5, the fraction is 70%; and for emissivity equal to 0.7, the fraction is 81%. For the different emissivities, the difference in the calculations shows up in the degree of melting in the plenum assembly. In addition to the melting of the end fittings and the guide structures, the bayonet tips of the leadscrews also would have been completely melted for the high and medium emissivity cases, and 95% melted for the lower emissivity case. The guide tubes below the 0.489-m elevation also are calculated to be melted in all three cases. One reason for this is that the hot gas is assumed to flow both on the inside and outside of the guide tubes below the 0.489 m elevation, thus increasing the heat transfer area. Another reason is that below the 0.489-m elevation, the 12 holes in a guide tube reduces the amount of mass per unit length of the guide tube. Above the 0.489 m elevation, the degree of melting of the guide tubes are different in the three cases: very little melting occurs in the low emissivity case, one-half melts in the medium emissivity case, and almost complete melting in the high emissivity case. For the leadscrews above the bayonet tips, the low emissivity case indicates that the average temperature would not have reached the melting point of steel, while the medium and high emissivity cases show partial and extensive melting, respectively.

The critical test in distinguishing between the low, medium, and high emissivity cases, based on up-to-date observations, lies in the degree of melting of the upper grid. At the end of 150 s, the high emissivity case produces too much melting (almost complete melting of the pads and about 40% of the grid ribs). The results of the medium emissivity case are within the observed bounds of the degree of melting for a few grid positions, but, overall, the calculated melting may still be too extensive compared with the observed damage. Finally, the low emissivity case predicts a degree of melting (22% for the pads and hardly any for the ribs) which is consistent with the observed average damage. The implication of the above comparisons is that the hot gas going through the upper plenum during the pump transient must have a substantial hydrogen content, which reduced the emissivity of the gas. This is in agreement with the deduction

from the thermal-hydraulic analysis given in Section 4.3. (The presence of hydrogen in the gas stream does not necessarily contradict the observation of foamy oxidation of steel. Oxidation of steel is precluded only if the hydrogen to steam ratio exceeds unity.[18])

The calculated amounts of material melted during the pump transient range from 1364 kg for the low emissivity case to about 2400 kg for the high emissivity case. About 940 kg of the melted material come from the end fittings. The molten material probably dripped into the core, through the upper core debris bed, and settled on top of the crust of the consolidated region. There is some evidence that the samples taken near the top crust are rich in iron, chromium, and nickel, much above their average contents in core composition.[17]

Section 4.3 gives an energy transfer of 30 GJ to the fluids during the pump transient. The energy transfer from the hot gas to the plenum assembly structures, however, is less than 2 GJ, as shown in Tables 4 through 6. Therefore, the heat transfer to the plenum assembly was only a minor thermal perturbation. This can also be seen from the slow decrease in gas temperature as a function of elevation. The gas temperature at 100 s (as a function of elevation for the low emissivity case)is shown in Figure 28. (Gas temperature distributions at other times and emissivities are similar to the one shown.)

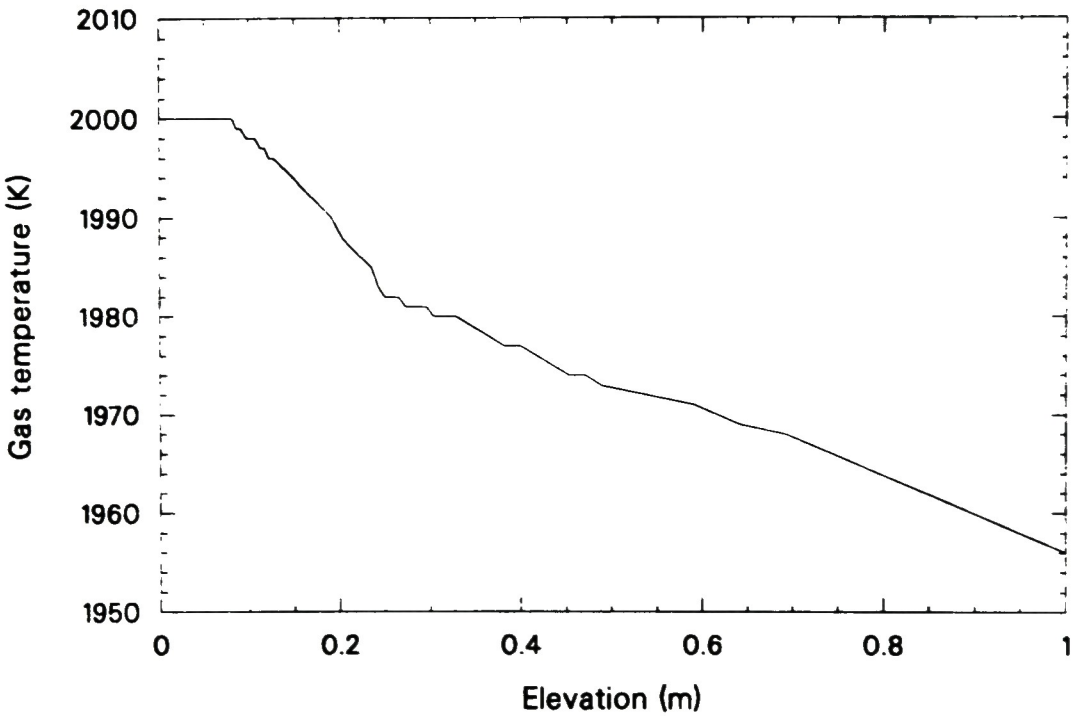

Figure 28. Calculated gas temperature distribution in the upper plenum during plenum assembly heating.

6. CONCLUSIONS

Since the first observation of the damage pattern on the underside of the TMI-2 plenum assembly in 1984, the damage mechanism has been somewhat a mystery. It has been generally understood that during the accident on March 28, 1979, hot gas flow from the reactor core ablated the structures at the lower end of the plenum assembly. During most of the core damage phase of the accident, the reactor coolant pumps were stopped. Therefore, natural circulation of hot gas between the core and upper plenum has been proposed as a mechanism that transferred heat from the core to the plenum assembly and caused the observed damage. To determine natural circulation patterns would require a multi-dimensional thermal-hydraulic code and a detailed model of the core and upper plenum. Such an endeavor has not been undertaken, and within the context of evaluating the TMI-2 accident, the tasks associated with such an endeavor seem monumental. The analyses presented in this report, though quite limited in scope, indicate that hot gas flow to the upper plenum during the 2-B primary coolant pump transient is a viable mechanism to satisfactorily explain the observed damage characteristics of the plenum assembly. In this concluding section, the bases and assumptions of the calculations are reviewed and the results of the calculations are compared with the observed damage. Any further work that could improve and refine the present calculations is also discussed.

There is little doubt that the observed damage on the underside of the plenum assembly was caused by thermal ablation of the structures during a period of high temperature gas flow. In the calculations, it was assumed that hot gas flowed past only the observed damage zones. Elsewhere, there was no hot gas flow and, hence, no damage. It was conjectured that because of the arrangement of the flow holes in the plenum cylinder, forced flow of hot gas from the core to the B-loop outlet nozzle was split into two streams, directed toward two regions in the north and the south quadrants of the upper plenum where damage to the plenum assembly occurred. Because of the removal of lateral resistance to fluid flow when the upper core collapsed at the time of the pump transient, the bifurcation of the flow stream would have developed below the lower surface of the plenum assembly.

The parameters entering the heat transfer calculations are the gas flow rate, gas temperature, and composition of the gas, which determines its thermal emissivity. The steam generation rate in the reactor core during the pump transient was calculated from the recorded pressure response. The steam flow rate to the upper plenum was equated to the steam generation rate in the reactor core, but the flow was directed to only the damaged regions of the plenum assembly. The amount of energy transferred to the fluid was larger than the amount of stored heat in the peripheral assemblies. It was concluded that the extra amount of energy must have come from the oxidation of zirconium which released hydrogen. From the characteristics of the debris bed of shattered fuel and cladding in the upper core, it was determined that the debris bed could not have been quenched during the short pump transient when limited amounts of water were introduced into the core. Instead, the debris bed must have been the source of the hot gas (a mixture of hydrogen and steam) which flowed toward the upper plenum. The temperature of the hot gas from the debris bed was assumed to be the same as the maximum average temperature attained by the particles. This temperature was determined to be about 2000 K, from examination of samples of the debris bed particles. The emissivity of the gas was taken as the only free parameter in the calculations, characterizing the amount of hydrogen present--the higher the hydrogen content, the lower the emissivity.

Hot gas generation during the pump transient lasted about 2-1/2 min. Based on the deduced flow rate and the assumed temperature, the results of the plenum assembly heating calculations, performed with a low thermal emissivity gas, i.e., a mixture of steam and hydrogen, agreed quite well with the observed extent of melting near the bottom of the plenum assembly. The thin structures, such as the internal structures of the end fittings and the control rod guide assemblies, would have been melted, and the relatively thick structures, such as the upper grid pads and ribs, would have been partially ablated. The amount of melted material is consistent with the tentative identification of an accumulation of iron, chromium, and nickel at the interface between the upper core debris bed and the top crust of the consolidated region in the damaged core.

The nonuniformity in plenum assembly damage within the observed damaged zones may be explained by the inhomogeneity of rapidly changing gas flow during the first 2-1/2 min of the pump transient. The fluctuating presence of hydrogen in the gas stream could explain the contrast between foamy steel oxidation and ablation without oxidation. However, characterization of these spatial and temporal fluctuations of the gas flow is beyond the scope of this study.

Although the calculations presented in this report strongly support a scenario that the plenum assembly was damaged during the 2-8 pump transient, there is much room to improve upon the calculations to unequivocally confirm the validity of the scenario. One obvious weakness in the calculational model is the assumption that hot gas flowed through only the observed damage zones. A multi-dimensional calculation could be performed for forced flow from the core to the upper plenum, using a model which would include the flow resistance of the control rod guide assemblies and taking into consideration the positions of the flow holes of the plenum cylinder. Because gas temperature would have a negligible effect on the flow pattern in forced flows, heat transfer to the structures could be ignored in forced flow calculations. These calculations would then be much simpler than natural circulation calculations and would be within the reach of present computing capabilities. The results of such calculations may confirm the flow bifurcation in the upper plenum and give better estimates of the mass flux of hot gas toward the damaged zones. Another area of improvement is the determination of the total fluid mass in the primary cooling system. As shown in Section 4.2, the steam generation during the pump transient, as computed from the recorded pressure history, depends on the total fluid mass present in the primary system. Ongoing TMI-2 Standard Problem calculations,[19] which follow the accident history from accident initiation to the pump transient, could narrow the range of fluid mass inventory estimates. Associated with the steam generation, one could also look into the hydrogen generation history. This would provide a basis to compute the time-dependent emissivity of the hot gas.

The thermal calculations show that the dominant heat transfer mode to the plenum assembly structures is thermal radiation. The calculations treat the radiative heat transfer in a rather crude way. Only radiative heat exchange between the gas and the structures is considered and this is limited to the directions perpendicular to the direction of flow. A proper treatment of the radiative heat transfer would involve the heat exchange among the structural elements and a consideration of the optical depth of the entire gas flow.

An undetermined factor in the thermal damage calculations is the temperature of the gas from the reactor core. The calculations in Section 5 used the peak average temperature determined for the particles in the upper core debris bed as the gas temperature. A first-principle determination of the gas temperature would involve modeling the interaction of the water delivered by the pump with the upper debris bed. Realistic modeling of such an interaction is beyond our present capabilities. However, the gas temperature is not a very sensitive parameter in determining the degree of ablation of the steel structures, so long as it is reasonably, say 100 K, over the melting point of steel. As the temperature increases, the emissivity of steam drops, making the increase in radiative heat flux and hence, the total heat flux less pronounced. It is likely that a higher temperature gas would be associated with a higher hydrogen content due to the oxidation of zirconium by steam, which supplies heat to drive up the temperature. This would also reduce the emissivity of the gas.

Despite the shortcomings discussed above (some of which can be remedied by refined models and calculations), the results of the simple calculations carried out in this study argue strongly for the 2-B primary coolant pump transient as the primary cause of the ablative damage observed on the plenum assembly underside.

7. REFERENCES

1. E. L. Tolman et al., TMI-2 Accident Scenario Update, EGG-TMI-7489, December 1986.

2. D. W. Akers et al., TMI-2 Core Debris Grab Samples--Examination and Analysis, GEND-INF-075, September 1986.

3. K. Vinjamuri, D. W. Akers, R. R. Hobbins, Examination of H8 and B8 Leadscrews from Three Mile Island Unit 2 (TMI-2), GEND-INF-052, September 1985.

4. M. Silbergerg et al., Reassessment of the Technical Bases for Estimating Source Terms, NUREG-0956, July 1986.

5. D. C. Wilson, TMI-2 Reactor Vessel Plenum Final Lift, GEND-054, January 1986.

6. M. R. Martin, private communication.

7. V. R. Fricke, "Results of End Fitting Separation in Preparation for Plenum Jacking," TMI-2 Technical Planning Bulletin, TPB-84-2, Rev. 0, November 9, 1984.

8. A. Takazawa ltr to J. M. Broughton, "Drawings of the Bottom Side of TMI-2 Upper Plenum," EG&G Idaho Interoffice Correspondence, AKI-1-85, October 23, 1985.

9. NSAC-80-1 (NSAC-1 Revised), Analysis of Three Mile Island - Unit 2 Accident, Nuclear Safety Analysis Center, Electric Power Research Institute, Palo Alto, California, March 1980.

10. J. L. Anderson, TMI-2 Once Through Steam Generator Secondary Level Analysis, EGG-TMI-7359, January 1987.

11. C. M. Allison et al., "SCDAP/RELAP5/MOD1 Code Manual," Volumes 1 and 2, DRAFT Preliminary Report, FIN No. A6360, February 1988.

12. D. W. Golden, private communication.

13. P. Kuan, TMI-2 Upper-Core Particle Bed Thermal Behavior, EGG-TMI-7757, August 1987.

14. W. H. McAdams, G. C. Williams, K. A. Smith, "Transmission of Heat by Conduction and Convection," Standard Handbook for Mechanical Engineers, T. Baumeister and L. S. Marks editing, Seventh Edition, McGraw-Hill, New York, 1967.

15. J. W. Spore et al., TRAC-BD1: An Advanced Best Estimate Computer Program for Boiling Water Reactor Loss-of-Coolant Accident Analysis, Volume 1: Model Description, NUREG/CR-2178, EGG-2109, October 1981.

16. C. W. Allen, Astrophysical Quantities, Second Edition, The Athlone Press, University of London, London, 1955.

17. D. W. Akers, private communication.

18. R. R. Hobbins et al., "Insights on Severe Accident Chemistry from TMI-2," Proceedings of the Symposium on Chemical Phenomena Associated with Radioactive Releases During Severe Nuclear Plant Accidents, NUREG/CP-0078, 1986.

19. E. L. Tolman et al., "TMI-2 Accident Evaluation Program," EGG-TMI-7048, February 1986.